Optics in a nonlinear gravitational wave

Abraham I. Harte

Max-Planck-Institut für Gravitationsphysik, Albert-Einstein-Institut
Am Mühlenberg 1, 14476 Golm, Germany

Abstract. Gravitational waves can act like gravitational lenses, affecting the observed positions, brightnesses, and redshifts of distant objects. Exact expressions for such effects are derived here, allowing for arbitrarily-moving sources and observers in the presence of plane-symmetric gravitational waves. The commonly-used predictions of linear perturbation theory are shown to be generically overshadowed—even for very weak gravitational waves—by nonlinear effects when considering observations of sufficiently distant sources; higher-order perturbative corrections involve secularly-growing terms which cannot necessarily be neglected. Even on more moderate scales where linear effects remain at least marginally dominant, nonlinear corrections are qualitatively different from their linear counterparts. There is a sense in which they can, for example, mimic the existence of a third type of gravitational wave polarization.

1. Introduction

Some of the most important potential signatures of gravitational waves are associated with their effects on the propagation of light. Collections of null rays can be deflected, sheared, delayed, or otherwise altered as they travel through a gravitational wave. Indeed, most contemporary attempts to observe gravitational waves rely on measurements of the relative time delays which accumulate as light travels between material bodies. This is particularly clear for interferometric detectors [1], where one or more beams of light are circulated between collections of mirrors and then recombined to reveal their relative phases. Efforts to detect gravitational waves using pulsar timing arrays [2] exploit similar principles, but instead make use of the times observed on the earth between radio bursts emitted by distant pulsars. Besides temporal effects such as these, gravitational waves can also affect observations of an object's sky location, brightness, shape, and so on [3, 4, 5, 6, 7, 8, 9].

Almost all prior discussions of these phenomena have been perturbative, involving calculations which are valid only through first order in the gravitational wave amplitude (see, however, [3, 10, 11, 12, 13]). This has been justified, at least implicitly, by the minuscule size of even these lowest-order terms: In most cases of astrophysical interest, the gravitational wave strain amplitude ϵ is much smaller than unity. Enormous technological effort is required to detect such waves at all, and precision measurements cannot be expected for quite some time. In this context, it might appear reasonable to dismiss higher-order corrections as uninterestingly-small. One of the goals of this paper is to show that such reasoning can be misleading. Even if a dimensionless observable associated with a gravitational wave of amplitude $\epsilon \ll 1$ is bounded by $\epsilon \times$ (number of order 1) in linear perturbation theory, higher-order corrections are not necessarily bounded by $\epsilon^2 \times$ (another number of order 1). The
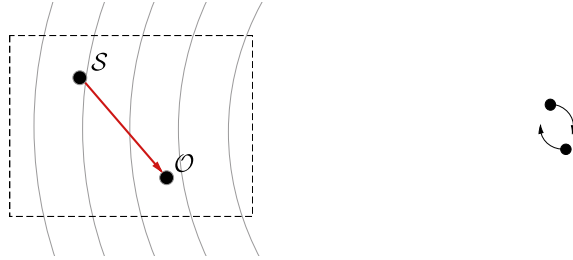
Figure 1: Schematic of a physical system which could correspond to the model considered in this paper. A "source" $\mathcal{S}$ emits electromagnetic radiation which is viewed by an "observer" $\mathcal{O}$. In between these objects, spacetime is assumed to be approximately flat except for a nearly-planar gravitational wave. This wave may be generated by a distant binary, although all considerations here are restricted to the boxed region, and are therefore indifferent to the precise nature of the wave generation mechanism.

coefficient in front of the ϵ^2 term can grow enormously with the distance between a light source and its observer, implying that nonlinearities may be significant even when considering observations of very weak gravitational waves. Nonlinear effects also tend to have very different observational signatures from their lower-order counterparts, further increasing their potential detectability.

Although it does not appear to have been previously pointed out in this context, the existence of large higher-order corrections is well-known in many types of perturbative calculations. A simple example is provided by the Mathieu-type equation

$$\ddot{\xi}(u) + \frac{1}{2}\epsilon\xi(u)\cos u = 0. \tag{1}$$

If u denotes an appropriate phase coordinate, $\xi^2(u)$ may be shown to describe a particular metric component associated with a linearly-polarized, "monochromatic" gravitational plane wave with strain amplitude ϵ. Moreover, the coordinate system where this is true is constructed such that there is a sense in which electromagnetic observations of distant objects have properties which can be read off directly from $\xi^2(u)$. Solutions to (1) therefore serve as a convenient proxy for understanding nonlinear effects associated with monochromatic gravitational waves in general relativity. Assuming $\epsilon \ll 1$ while adopting convenient initial conditions,

$$\xi^2(u) = 1 + \epsilon\cos u + \frac{1}{8}\epsilon^2(3\cos^2 u - u^2) + O(\epsilon^3). \tag{2}$$

The magnitude of the second-order term in this expansion clearly overtakes the first when $|u| \sim \epsilon^{-1/2} \gg 1$, signaling that the linear approximation fails for large $|u|$. This occurs no matter how small ϵ may be; weaker amplitudes merely delay such problems to larger scales.

We show that similar effects arise for a variety of gravitational wave observables, thus implying that the results of linear perturbation theory cannot necessarily be applied directly on large scales. As a model, geometric optics is considered in the presence of a plane-symmetric gravitational wave. The waveform and polarization content of this wave is unconstrained, and all optical elements—the observers and the observed—are allowed to move arbitrarily. Such systems may be viewed as idealizations of the one illustrated in Figure 1, where observations are performed

sufficiently far from a gravitational wave source that the curvature of the wavefronts can be neglected. Similar models, though restricted only to first-order metric perturbations, are common in, e.g., the literature describing how gravitational waves affect pulsar timing measurements [2, 14].

Despite this, real astrophysical observations cannot rely solely upon plane wave calculations. Deviations from planarity, waves propagating in multiple directions, non-radiative metric perturbations, and other effects might all be relevant. Calculations which take into account many such possibilities have indeed been performed through first post-Minkowskian order [7, 15]. Although some partial results on optical effects in realistic astrophysical systems have been found even through second post-Minkowskian order [16, 17], essentially nothing seems to be known regarding nonlinear gravitational waves in these settings. Moreover, it would likely be difficult to explore the implications of any such formulae even if they did exist; the known first-order expressions are already extremely complicated in their most general forms. Plane waves are, by contrast, sufficiently simple that their physical effects *can* be thoroughly explored. At the same time, these waves also appear to capture much of the relevant physics. Results obtained using plane wave descriptions may therefore be useful in the construction of specific hypotheses whose generality can later be tested using more complicated models. The technical details of the plane wave problem can also be used to suggest potential simplifications in more general calculations.

A completely separate motivation for considering plane wave spacetimes follows from a mathematical device known as the Penrose limit [18, 19, 20]. This provides a sense by which the geometry near any null geodesic in any spacetime is equivalent to the geometry of an appropriate plane wave. It can be interpreted as a statement that the metric in a small region around any sufficiently-relativistic observer in any spacetime is equivalent to that of an "effective plane wave." Although we make no attempt to prove it, the Penrose limit suggests that (at least some types of) observations performed by ultrarelativistic observers can *in general* be reduced to analogous observations in effective plane wave spacetimes.

Section 2 reviews gravitational plane waves in general relativity, first from the viewpoint of perturbation theory, and then as exact solutions to Einstein's equation. Relations between these two perspectives and their relative advantages are described in detail. Section 3 considers the physical consequences of plane wave spacetimes by deriving exact time delays, frequency shifts, observed sky positions, area distances, and luminosity distances. With appropriate identifications, some of the resulting expressions are only slightly more complicated than their linearized counterparts. Formal perturbative expansions are nevertheless derived in Section 4 and then applied to specific examples in Section 5.

Notation and conventions

The metric signature here is $+2$, $c = G = 1$, the Riemann tensor satisfies $R_{abc}{}^d \omega_d = 2\nabla_{[a}\nabla_{b]}\omega_c$ for any ω_c, Latin letters $a, b, \ldots$ denote abstract indices, Greek letters $\mu, \nu, \ldots$ denote four-dimensional coordinate indices, and $i, j, \ldots$ are used as two-dimensional coordinate indices associated with directions transverse to the background gravitational wave. When convenient, transverse coordinate components are indicated using boldface symbols without indices [e.g., $\gamma_{ij} = (\boldsymbol{\gamma})_{ij}$, $\gamma_{ij} w^i v^j = \boldsymbol{w}^{\mathsf{T}} \boldsymbol{\gamma} \boldsymbol{v}$, and $\operatorname{tr} \boldsymbol{\gamma} = \delta_{ij} \gamma_{ij}$]. Overdots are used to denote derivatives with respect to a phase coordinate u, so $\dot{\gamma}_{ij} = \mathrm{d}\gamma_{ij}/\mathrm{d}u$.

2. Gravitational plane waves

Before describing how light propagates in a gravitational plane wave, it must first be explained precisely what a plane wave is. Although the concept is clear for a scalar field in flat spacetime, subtleties arise when considering curved geometries or fields with nontrivial tensorial structure. This difficulty is reflected in part by the two distinct perspectives on gravitational plane waves—one perturbative and one exact— which are common in the literature. While both of these perspectives are individually well-known, the relations between them are not. This section clarifies the situation, and also remarks on special types of plane waves.

2.1. Approximate plane waves

Almost every textbook on general relativity discusses gravitational waves as linear perturbations on a flat background spacetime [21, 22]. To review, suppose that there exist coordinates (t, x^1, x^2, z) in which the metric components can be approximated by $g_{\mu\nu} = \eta_{\mu\nu} + \epsilon h_{\mu\nu} + O(\epsilon^2)$, where $\epsilon \ll 1$ is a dimensionless expansion parameter and $\eta_{\mu\nu}$ is the Minkowski metric. It is also typical to adopt the transverse-traceless, or "TT" gauge, in which case $h_{\mu t} = \eta^{\mu\nu} h_{\mu\nu} = \eta^{\mu\nu} \partial_\mu h_{\nu\lambda} = 0$. These constraints on the metric perturbation can always be imposed in connected regions of spacetime where the linearized vacuum Einstein equation holds [23]. Imposing TT gauge in such a region, the first-order vacuum Einstein equation reduces there to the ordinary flat-spacetime wave equation for each coordinate component of the perturbation: $(-\partial_t^2 + \nabla^2)h_{\mu\nu} = 0$.

The solutions of interest here represent plane-symmetric gravitational waves propagating in vacuum. If the spatial projection of a plane wave's direction of propagation is identified with $\partial/\partial z$, the only components of the metric perturbation which might not vanish are h_{ij}, where $i = 1, 2$. This 2×2 symmetric matrix must be trace-free, and can depend only on the "phase coordinate" $u = (t - z)/\sqrt{2}$. The first-order line element for an arbitrary plane wave propagating in the z-direction is therefore

$$\mathrm{d}s^2 = -\mathrm{d}t^2 + [\delta_{ij} + \epsilon h_{ij}(u)]\mathrm{d}x^i \mathrm{d}x^j + \mathrm{d}z^2 + O(\epsilon^2), \tag{3}$$

where

$$\boldsymbol{h}(u) = \begin{pmatrix} h_+(u) & h_\times(u) \\ h_\times(u) & -h_+(u) \end{pmatrix}, \tag{4}$$

and $h_+(u)$, $h_\times(u)$ represent the waveforms associated with the "+" and "×" polarization states. A plane wave is said to be linearly polarized if $h_\times$ (or h_+) can be made to vanish via some constant rotation of the x^1, x^2 coordinates.

2.2. Exact plane waves

The exact theory of gravitational plane waves is often presented very differently from its linearized counterpart. One way to motivate an exact plane wave solution in general relativity is to first search for those geometries which share—independently of Einstein's equation—the symmetries associated with more familiar plane waves in flat spacetime. Consider, for example, a scalar field with the form $f = f(t - z)$ in special relativity. This is clearly symmetric with respect to the two spacelike translations

$\partial/\partial x^i$ and the single null translation $\partial/\partial t + \partial/\partial z$. Less obviously, scalar plane waves are also preserved by

$$\left(x^i \frac{\partial}{\partial z} - z \frac{\partial}{\partial x^i} \right) + \left(x^i \frac{\partial}{\partial t} + t \frac{\partial}{\partial x^i} \right), \tag{5}$$

two Killing vector fields which generate rotations in the x^i-z planes combined with boosts along the x^i directions. It follows that scalar plane waves in flat spacetime are preserved by at least five Killing vector fields associated with the geometry through which they propagate. The same symmetries also preserve electromagnetic plane waves in flat spacetime, thus motivating a gravitational plane wave in four dimensions as a curved spacetime which admits at least five linearly-independent Killing vector fields [24]. The resulting metrics are most commonly-stated in terms of the so-called Brinkmann coordinates (U, V, X^1, X^2), in which case

$$\mathrm{d}s^2 = -2\mathrm{d}U\mathrm{d}V + H_{ij}(U)X^iX^j\mathrm{d}U^2 + (\mathrm{d}X^1)^2 + (\mathrm{d}X^2)^2. \tag{6}$$

Using this as an ansatz, the *exact* vacuum Einstein equation reduces to

$$\operatorname{tr}\boldsymbol{H} = 0. \tag{7}$$

Any 2×2 symmetric trace-free matrix $H_{ij}(U)$ therefore describes an exact plane wave in vacuum general relativity. We call this the Brinkmann waveform. Its two independent components correspond to the two possible polarization states of a gravitational wave in vacuum general relativity. The Brinkmann waveform has a direct geometric significance in the sense that the only independent, non-vanishing curvature components are

$$R_{UiUj} = -H_{ij}. \tag{8}$$

Up to ambiguities in the construction of the coordinate components R_{UiUj}, this waveform can therefore be obtained using only local measurements. Such ambiguities are minor, and can be taken into account using only three constants c_b, c_r, and c_t [25]. Explicitly, two waveforms are physically identical if and only if they can be related via the complex replacement rule

$$H_{11}(U) + iH_{12}(U) \to c_b^2 [H_{11}(c_b U - c_t) + iH_{12}(c_b U - c_t)]e^{ic_r}, \tag{9}$$

where $c_b \neq 0$ describes a constant boost along the direction of propagation, c_t a constant translation of the phase coordinate U, and c_r a constant rotation. This is sufficiently simple that it is typically evident by inspection whether or not two Brinkmann waveforms describe the same physical system.

Physically, a plane wave described by the metric (6) propagates in the null direction $\ell^a = \partial/\partial V$. Up to an overall constant, ℓ^a is the unique nonvanishing vector field which is both null and covariantly constant in any curved region of a plane wave spacetime. Noting that $\ell_a = -\nabla_a U$, these constraints define the U coordinate up to an overall affine transformation. It may be interpreted as the phase of the gravitational wave. Interpretations of the remaining Brinkmann coordinates follow by noting that they form a kind of Fermi normal coordinate system whose "origin" is the null geodesic $V = X^i = 0$ [19].

Plane waves are extremely simple when described in terms of Brinkmann waveforms. It is clear from (7) that if $H_{ij}(U)$ and $H'_{ij}(U)$ are any two vacuum waveforms, $H_{ij}(U) + H'_{ij}(U)$ is also a vacuum waveform. This provides a sense by which plane waves in general relativity satisfy exact linear superposition; there is no nonlinearity to speak of. Superpositions of this type are special cases of the more

general result that the vacuum Einstein equation is linear for all metrics within the Kerr-Schild class. More precisely, suppose that there exists some null $\hat{\ell}_a$ and some scalar $\mathcal{H}$ such that $g_{ab} = \hat{g}_{ab} + \mathcal{H}\hat{\ell}_a\hat{\ell}_b$ is an exact solution to the vacuum Einstein equation for some vacuum "background" $\hat{g}_{ab}$. If $g'_{ab} = \hat{g}_{ab} + \mathcal{H}'\hat{\ell}_a\hat{\ell}_b$ is a second exact solution, the metric $g''_{ab} = \hat{g}_{ab} + (\mathcal{H} + \mathcal{H}')\hat{\ell}_a\hat{\ell}_b$ must be an exact solution as well [26]. For the plane wave case of interest here, the Kerr-Schild decomposition is recovered by letting $\hat{\ell}_a = \ell_a = -\nabla_a U$ and $\mathcal{H} = H_{ij}X^iX^j$, in which case $\hat{g}_{ab}$ is flat. Waveforms of this type are very special, and the linearity of Einstein's equation which they make manifest is not at all apparent if plane waves are parametrized using different variables. Nevertheless, the optical observables discussed below are more conveniently described in terms of different waveforms which i) generalize the perturbative h_{ij} appearing in (3), and ii) do not satisfy linear superposition.

2.3. Relating the exact and approximate descriptions

Although the TT-gauge metric (3) describes, at least approximately, the same physical system as the Brinkmann metric (6), the former expression is not a trivial linearization of the latter. Understanding how these two descriptions relate to one another requires an appropriate coordinate transformation. The TT gauge makes sense only at first perturbative order, so a non-perturbative generalization of this gauge must be sought. We choose to employ those transformations which preserve, in an appropriate sense, the TT-gauge property that objects at "fixed spatial coordinates" move on timelike geodesics. Additionally, we require that the planar symmetry of the metric be manifest in the sense that there exist two coordinates x^i, interpreted as parametrizing the 2-surfaces transverse to the gravitational wave, such that the vector fields $\partial/\partial x^i$ are both spacelike and Killing. These constraints are chosen not merely to facilitate a simple translation between the perturbative and non-perturbative viewpoints. Much more importantly, it is shown in Section 3 below that the "TT-like" coordinates which they define are particularly well-adapted to describing optical observables in the presence of a gravitational wave.

The appropriately-generalized TT coordinates are denoted here by (u, v, x^1, x^2). They are known in the literature as Rosen coordinates, and are related to their Brinkmann counterparts (U, V, X^1, X^2) via

$$u = U, \quad \boldsymbol{x} = \boldsymbol{\xi}^{-1}(U)\boldsymbol{X}, \quad v = V - \frac{1}{2}[\dot{\boldsymbol{\xi}}(U)\boldsymbol{\xi}^{-1}(U)]_{ij}X^iX^j, \qquad (10)$$

where $\xi_{ij}(U)$ is any nonsingular 2×2 (not necessarily symmetric) matrix satisfying

$$\ddot{\boldsymbol{\xi}}(U) = \boldsymbol{H}(U)\boldsymbol{\xi}(U), \qquad (\boldsymbol{\xi}^{\mathsf{T}}\dot{\boldsymbol{\xi}})_{[ij]} = 0. \qquad (11)$$

Any ξ_{ij} with these properties is essentially a Jacobi propagator: Contracting it on the right with an arbitrary constant vector results in the nontrivial components of a solution‡ to the geodesic deviation (or Jacobi) equation [20]. Given any such propagator with the specified properties, the exact plane wave metric (6) becomes

$$ds^2 = -2dudv + \gamma_{ij}(u)dx^idx^j, \qquad (12)$$

‡ The geodesic deviation equation may be written as $\ddot{\boldsymbol{\psi}} = -\boldsymbol{R}\boldsymbol{\psi}$ *in any spacetime*, where $\boldsymbol{\psi}$ denotes the four-dimensional deviation vector resolved into parallel-propagated tetrad components, $\boldsymbol{R}$ is a 4×4 matrix of similarly-decomposed Riemann components, and overdots represent ordinary derivatives with respect to an affine parameter [27].

where

$$\gamma_{ij}(u) = \gamma_{(ij)}(u) \equiv \xi_{ki}(u)\xi_{kj}(u). \tag{13}$$

The implied summation in this last equation is understood to be trivial in the sense that $\gamma_{ij} = \sum_k \xi_{ki}\xi_{kj}$, or equivalently $\boldsymbol{\gamma} = \boldsymbol{\xi}^{\mathsf{T}}\boldsymbol{\xi}$. The Rosen line element (12) naturally splits into a longitudinal component $-2\mathrm{d}u\mathrm{d}v$ and a transverse component $\gamma_{ij}(u)\mathrm{d}x^i\mathrm{d}x^j$. The longitudinal portion is flat and Lorentzian, while the transverse portion is associated with the Riemannian 2-metric $\gamma_{ij}(u)$. We often refer to this 2-metric as the Rosen waveform. It depends only on the phase u of the gravitational wave, and is related to the Brinkmann waveform $H_{ij}(U)$ via (11) and (13).

That the Rosen coordinates are, as claimed, a type of geodesic normal coordinate system may be verified by noting that every fixed-x^i 2-surface contains a timelike geodesic. Moreover, each such surface actually contains a 1-parameter family of timelike geodesics related by longitudinal boosts. It also contains a null geodesic along which $v = (\text{constant})$. These statements can be made more intuitive in terms of the quasi-Cartesian coordinates

$$t = \frac{1}{\sqrt{2}}(v + u), \qquad z = \frac{1}{\sqrt{2}}(v - u), \tag{14}$$

defined by analogy with standard null $\to$ inertial transformations in flat spacetime. The vector $\partial/\partial z$ is now a spatial projection of the wave propagation direction ℓ^a. Additionally, any worldline which remains at fixed (x^i, z) is a timelike geodesic. More generally, all curves satisfying $\mathrm{d}x^i/\mathrm{d}t = 0$ and $|\mathrm{d}z/\mathrm{d}t| = (\text{constant}) < 1$ are timelike geodesics. Worldlines constrained by $\mathrm{d}x^i/\mathrm{d}t = 0$, $|\mathrm{d}z/\mathrm{d}t| = 1$ are instead null geodesics. These statements imply that a large class of geodesics are trivial in terms of Rosen coordinates. Geodesics which are not in this class can appear quite complicated, however. A generic timelike geodesic may be specified by choosing initial conditions for its transverse components at some fiducial phase $u = u_0$, as well as a constant $\lambda > 0$ which describes motion longitudinal to the wave. Defining the phase average of the inverse 2-metric by

$$\langle \boldsymbol{\gamma}^{-1} \rangle \equiv \frac{1}{u - u_0} \int_{u_0}^{u} \boldsymbol{\gamma}^{-1}(\tau)d\tau, \tag{15}$$

an arbitrary timelike geodesic may be shown to have the coordinate parametrization

$$\boldsymbol{x}(u) = \boldsymbol{x}(u_0) + (u - u_0)\langle \boldsymbol{\gamma}^{-1} \rangle \boldsymbol{\gamma}(u_0)\dot{\boldsymbol{x}}(u_0), \tag{16}$$

$$v(u) = v(u_0) + (u - u_0)\left(\lambda^2 + \frac{1}{2}[\boldsymbol{\gamma}(u_0)\langle \boldsymbol{\gamma}^{-1} \rangle \boldsymbol{\gamma}(u_0)]_{ij}\dot{x}^i(u_0)\dot{x}^j(u_0)\right). \tag{17}$$

Geodesics which remain at fixed (x^i, z) satisfy $\dot{x}^i(u_0) = 0$ and $\lambda = 1$.

That the Rosen metric directly generalizes the TT-gauge plane wave (3) follows from applying (14) to (12), which produces the exact line element $\mathrm{d}s^2 = -\mathrm{d}t^2 + \gamma_{ij}(u)\mathrm{d}x^i\mathrm{d}x^j + \mathrm{d}z^2$. Standard perturbative results are therefore recovered if

$$\gamma_{ij} = \delta_{ij} + \epsilon h_{ij} + O(\epsilon^2) \tag{18}$$

and $\mathrm{tr}\,\boldsymbol{h} = 0$. It is shown in Section 4.1 that such expansions do indeed arise when considering smooth 1-parameter families of plane wave spacetimes. While the vacuum Einstein equation is both linear and algebraic in terms of H_{ij} [cf. (7)], it is a nonlinear differential equation when expressed in terms of γ_{ij}. This means that the $O(\epsilon^2)$ terms neglected in (18) are generically nontrivial. They may be interpreted as corrections

due to the higher-order Einstein equation, or alternatively as higher-order solutions to a family of geodesic equations.

This latter perspective follows from the interpretation of Rosen coordinates as a lattice of timelike geodesics. The relative displacements of these geodesics are encoded in γ_{ij}. Remarkably, this matrix also encodes in a simple way many properties of the *null* geodesics which are so central to the calculations of geometric optics. Plane wave spacetimes are sufficiently simple that most of the information required to characterize the propagation of light can i) be embedded in the Rosen-coordinate metric components, and ii) this coordinate choice is one for which considerable intuition and experience already exists (at least perturbatively). For these reasons, the remainder of this paper works almost exclusively in Rosen coordinates.

More precisely, we suppose that a *particular* Rosen coordinate system has been chosen. The relations between the Brinkmann waveform H_{ij} and the Rosen waveform γ_{ij} are both nonlocal and nonunique, meaning that even if a single Brinkmann coordinate system is fixed, the transformation (10) allows for many different Rosen coordinate systems. Different solutions to (11) are possible, and different resulting solutions for ξ_{ij} generically define different γ_{ij} via (13). This freedom corresponds to the ability to choose different collections of timelike geodesics as coordinate markers. It can be described more precisely as the set of all solutions to $\ddot{\boldsymbol{\xi}} = \boldsymbol{H}\boldsymbol{\xi}$ for which $\boldsymbol{\xi}^{\mathsf{T}}\dot{\boldsymbol{\xi}}$ is symmetric (a constraint which is true everywhere if it is true anywhere), and for which $\boldsymbol{\gamma} = \boldsymbol{\xi}^{\mathsf{T}}\boldsymbol{\xi}$ is nonsingular, modulo those solutions which preserve $\boldsymbol{\xi}^{\mathsf{T}}\boldsymbol{\xi}$. Fixing a particular H_{ij} while choosing a fiducial phase u_0, any two such solutions ξ_{ij}, ξ'_{ij} to (11) must be related by

$$\boldsymbol{\xi}'(u) = \boldsymbol{\xi}(u) \left\{ \boldsymbol{\xi}^{-1}(u_0)\boldsymbol{\xi}'(u_0) + (u - u_0)\langle\boldsymbol{\gamma}^{-1}\rangle \left[\boldsymbol{\xi}^{\mathsf{T}}(u_0)\dot{\boldsymbol{\xi}}'(u_0) - \dot{\boldsymbol{\xi}}^{\mathsf{T}}(u_0)\boldsymbol{\xi}'(u_0) \right] \right\}. \quad (19)$$

The complexity of this relation makes it clear that if one is presented with two Rosen waveforms γ_{ij}, γ'_{ij}, it not necessarily obvious by inspection whether or not they describe the same spacetime. It is nevertheless possible to check equivalence by computing some ξ_{ij} and ξ'_{ij} which generate the appropriate waveforms, and then determining if $\ddot{\boldsymbol{\xi}}\boldsymbol{\xi}^{-1}$ and $\ddot{\boldsymbol{\xi}}'\boldsymbol{\xi}'^{-1}$ can be related by the transformation (9).

Although it is rarely discussed, the same ambiguities regarding representations of gravitational waves arise even in the linearized theory. As a possible counterpoint, one might object that vacuum, first-order, TT-gauge metric perturbations on a flat background are known to be invariant with respect to first-order gauge transformations. Such statements depend, however, on global assumptions such as asymptotic falloff (cf. Section 2.3 of [23]). If a spacetime is taken to be a literal plane wave, there is no such falloff. If, more realistically, a plane wave is used only as a model intended to be valid in a finite region of spacetime, the true asymptotic boundary conditions are external to the modeled region and therefore unusable. From either perspective, the familiar uniqueness of TT-gauge metric perturbations is lost. If (18) holds, the transformations $h_{ij}(u) \rightarrow h_{ij}(u) + c_{ij} + u d_{ij}$ are easily shown to describe the same geometry through $O(\epsilon)$ for any constant trace-free matrices c_{ij}, d_{ij}.

We assume that a particular Rosen coordinate system has been chosen such that $\det \boldsymbol{\xi} > 0$ everywhere of interest. This ensures that a single coordinate patch can be used in all calculations, and also that the orientations of the x^i and X^i coordinates are identical. As with all geodesic-type coordinate systems, gravitational focusing generically causes Rosen coordinate systems to break down on sufficiently large scales. Restricting to a single coordinate patch therefore implies an upper bound on the maximum distances over which the calculations described here can be applied. This

bound is, for example, of order $(\epsilon\omega)^{-1}$ in the case of a monochromatic gravitational wave with angular frequency ω and strain amplitude ϵ. Optical effects involving larger scales are discussed in [3].

2.4. Rosen metrics: Non-perturbative considerations

Suppose that a particular vacuum plane wave has been fixed by prescribing a trace-free matrix $H_{ij}(u)$. This is equivalent, via (8), to prescribing the wave's curvature. Rosen waveforms then follow from (11) and (13), implying that $\gamma_{ij}(u)$ is essentially the square of a matrix which describes the displacements of coupled parametric oscillators attached to "springs" whose squared natural frequencies are proportional to $H_{ij}(u)$. Similar equations arise throughout physics and engineering, and a variety of methods have been developed to understand them.

A large class of physically-relevant waveforms can be classified as either "burstlike"—having a large amplitude only for a short time—or "continuous," implying approximate periodicity. The curvature associated with a burst might be further idealized as vanishing completely whenever u lies outside a bounded connected region $\mathcal{C} \subset \mathbb{R}$. The spacetime can then be viewed as a curved region sandwiched between two flat connected regions $\mathcal{F}_\pm$. Such spacetimes are often described as "sandwich waves." In either of the flat regions where $H_{ij} = 0$, the general solution to (11) is

$$\boldsymbol{\xi}(u) = \boldsymbol{a}_{\mathcal{F}_\pm} + u\boldsymbol{b}_{\mathcal{F}_\pm}, \tag{20}$$

The two matrices $\boldsymbol{a}_{\mathcal{F}_\pm}$, $\boldsymbol{b}_{\mathcal{F}_\pm}$ must be constant and must satisfy $(\boldsymbol{a}_{\mathcal{F}_\pm}^\mathsf{T} \boldsymbol{b}_{\mathcal{F}_\pm})_{[ij]} = 0$ and $\det(\boldsymbol{a}_{\mathcal{F}_\pm} + u\boldsymbol{b}_{\mathcal{F}_\pm}) > 0$ everywhere of interest.

The trivial case of a spacetime which is everywhere flat is conventionally described by a metric in which $\gamma_{ij} = \delta_{ij}$, implying that ξ_{ij} must be a constant orthogonal matrix. This is not required, however. Regions of flat spacetime can also be covered by coordinate systems whose "waveforms"—computed as squares of expressions like (20)—grow quadratically with u. Recalling (6) and (10), this corresponds to using non-comoving geodesics as coordinate markers. Such possibilities are an uninteresting complication in Minkowski spacetime. They can, however, be unavoidable when considering bursts of gravitational waves. While it is always possible to choose, say, $\boldsymbol{a}_{\mathcal{F}_-} = \boldsymbol{I}$ and $\boldsymbol{b}_{\mathcal{F}_-} = 0$ in one flat region $\mathcal{F}_-$ of a sandwich wave, fixing these constants removes any freedom to additionally specify $\boldsymbol{a}_{\mathcal{F}_+}$ and $\boldsymbol{b}_{\mathcal{F}_+}$. The latter matrices must be determined by integrating (11) through the intervening curvature. Choosing $\gamma_{ij} = \delta_{ij}$ in $\mathcal{F}_-$ therefore does not guarantee that the same relation holds in $\mathcal{F}_+$. Nontrivial differences between the "before" and "after" Rosen waveforms are manifestations of the gravitational memory effect. Waves with memory are discussed in more detail in Sections 4.1.1 and 5.2 below.

Plane waves which cannot be modeled as bursts, but whose curvature is instead periodic in u, may be understood using different methods. In these cases, $\ddot{\boldsymbol{\xi}} = \boldsymbol{H}\boldsymbol{\xi}$ corresponds to a set of coupled Hill-like equations. Although some methods exist for finding exact solutions to Hill equations [28, 29], these are rather limited. General properties of periodic waves may instead be understood using Floquet theory [30]. It follows from this that even though ξ_{ij} and $\gamma_{ij} = \xi_{ki}\xi_{kj}$ do not typically share the periodicity of H_{ij}, knowledge of ξ_{ij} in only one oscillation period can be used to construct it everywhere. Although we shall not do so here, such methods can be used to greatly enlarge the validity of perturbative calculations. It also follows from
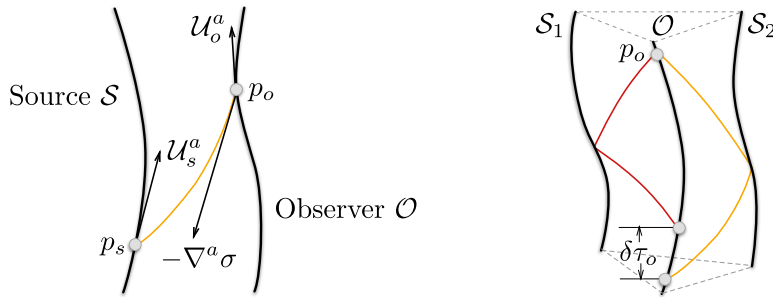
(a) Diagram illustrating the observation of a pointlike source $\mathcal{S}$ by an observer $\mathcal{O}$. The observation event p_o is connected to the emission event p_s by a light ray whose tangent can be computed as the gradient of Synge's function σ. Source and observer 4-velocities are denoted by $\mathcal{U}_{o,s}^a$.

(b) A two-arm interferometer with an observer $\mathcal{O}$ flanked by two mirrors $\mathcal{S}_{1,2}$. The relative phases of the light compared at p_o determine the difference $\delta\tau_o$ in their emission times. This system may be viewed as a composite the one in part (a).

Floquet theory that some waves are unstable in the sense that there exist $\xi_{ij}(u)$ which grow exponentially with increasing u. Dramatic effects like these require very large gravitational wave amplitudes, and are not discussed any further here.

3. Non-perturbative optical observables

Locally, one obvious observable in any spacetime is its curvature $R_{abc}{}^d$. This is directly relatable in plane wave spacetimes to the Brinkmann waveform H_{ij} via (8), and can always be obtained [up to transformations with the form (9)] from local measurements. Understanding a spacetime through its effects on the appearance of distant objects can be considerably more complicated, depending in general on the spacetime structure throughout extended regions, and also on the motions of any material objects which may be involved.

This section considers the effects of gravitational plane waves on the propagation of light in the geometric optics approximation. If a distant source is observed through an intervening plane wave, its spectrum, apparent location, angular size, and brightness can all be affected. Some (though not all) of these effects have been considered previously in [3], but in terms of Brinkmann coordinates. The resulting expressions were difficult to interpret, and could not be immediately compared to existing perturbative results. The expressions derived here are far simpler both to understand and to apply.

The main system we consider is illustrated in Figure 2a. There, a source is abstracted to a timelike worldline $\mathcal{S}$ and its observer to another timelike worldline $\mathcal{O}$. Images then correspond to past-directed null geodesics from $\mathcal{O}$ to $\mathcal{S}$. Given any observation event $p_o \in \mathcal{O}$, exactly one image is assumed to exist in all cases considered here§. The remainder of this paper explores the properties of these images. More complicated optical problems (such as the interferometer illustrated in Figure 2b) can

§ There exist special source-observer configurations where pointlike sources appear as extended images. Plane wave spacetimes can also admit multiple discrete images on very large scales which cannot be described by the single Rosen coordinate patch assumed here [3, 12, 34].

typically be understood as multiple instances of system shown in Figure 2a. All results in this section are exact. Unless otherwise indicated, no restrictions are placed on the motions of the source or the observer.

3.1. Time of flight

Observations such as those illustrated in Figure 2a provide a natural mapping between "observation times" and "emission times." More precisely, the light rays which connect $\mathcal{S}$ to $\mathcal{O}$ may be used to relate the proper time τ_o recorded by $\mathcal{O}$ at an observation event $p_o \in \mathcal{O}$ to the proper time τ_s recorded by $\mathcal{S}$ at the emission event $p_s \in \mathcal{S}$. Such relations play an important role in all optical calculations performed below. The redshift or blueshift can, for example, be computed from $\mathrm{d}\tau_s/\mathrm{d}\tau_o$. Additionally, the time difference $\delta\tau_o$ (or the phase shift) for the interferometer illustrated in Figure 2b follows by successively applying the maps $\tau_s(\tau_o)$ applicable to each pair of optical elements.

As a first step towards computing $\tau_s(\tau_o)$ for the simpler system in Figure 2a, consider instead the gravitational wave phase $u_s(u_o)$ at p_s as a function of the gravitational wave phase u_o at p_o. Although the plane wave phase coordinate u is null, the difference $u_o - u_s(u_o)$ may nevertheless be interpreted as a "time of flight" for a photon traveling from $\mathcal{S}$ to $\mathcal{O}$. This interpretation is supported by noting that i) the u coordinate is unique up to a constant affine transformation, and ii) the restriction of u to any timelike geodesic is, up to a positive constant, a proper time for that geodesic.

The phase relation $u_s(u_o)$ can be computed using Synge's function $\sigma(p, p')$. This is a two-point scalar which takes two events as arguments and returns one-half the squared geodesic distances between those events [27, 31, 32]. Plane wave spacetimes are one of the few examples where this function is known explicitly (although generic post-Minkowskian approximations are available [33]), with the Brinkmann form appearing in, e.g., [20] and the Rosen form in [32]. Given two events p, p' and their associated Rosen coordinates,

$$\sigma(p, p') = -(u - u')(v - v') + \frac{1}{2}[\langle\boldsymbol{\gamma}^{-1}\rangle^{-1}]_{ij}(x - x')^i(x - x')^j. \quad (21)$$

The average $\langle\boldsymbol{\gamma}^{-1}\rangle$ appearing here is the same as in (15), except that it is to be evaluated between u' and u instead of between u_0 and u. For the trivial case of a spacetime which is globally-flat, there exist coordinates where $\gamma_{ij} = \delta_{ij}$ and so $\sigma_{\text{flat}}(p, p') = -(u - u')(v - v') + \frac{1}{2}|\boldsymbol{x} - \boldsymbol{x}'|^2 = \frac{1}{2}[-(t - t')^2 + |\boldsymbol{x} - \boldsymbol{x}'|^2 + (z - z')^2]$. The general expression (21) for the geodesic distance in an arbitrary plane wave differs from this only via the replacement $\boldsymbol{I} \to \langle\boldsymbol{\gamma}^{-1}\rangle^{-1}$ in the transverse directions.

The existence of the null geodesic which connects the observation and emission events illustrated in Figure 2a implies that

$$\sigma(p_o, p_s) = \sigma(p_s, p_o) = 0, \quad (22)$$

so

$$u_o - u_s = \frac{1}{2}(v_o - v_s)^{-1}[\langle\boldsymbol{\gamma}^{-1}\rangle^{-1}]_{ij}(x_o - x_s)^i(x_o - x_s)^j \quad (23)$$

whenever $v_s \neq v_o$. Using the t and z coordinates defined by (14) instead results in the equivalent

$$t_o - t_s = \sqrt{[\langle\boldsymbol{\gamma}^{-1}\rangle^{-1}]_{ij}(x_o - x_s)^i(x_o - x_s)^j + (z_o - z_s)^2}. \quad (24)$$

Supplementing these equations with appropriate parametrizations for the source coordinates in terms of the gravitational wave phase allows explicit solutions to be obtained for $u_s(u_o)$ or $t_s(t_o)$. If the source and observer move on geodesics, the necessary parametrizations are given by (16) and (17).

Once $u_s(u_o)$ is known, it may be used to relate proper times associated with the observation and emission events. The observer's proper time τ_o is related to the gravitational wave phase via

$$\frac{\mathrm{d}\tau_o}{\mathrm{d}u} = -\frac{1}{\mathcal{U}_o^a \ell_a}, \tag{25}$$

where $\mathcal{U}_o^a$ denotes the observer's 4-velocity and $\ell^a = \partial/\partial v$ the gravitational wave's propagation direction. Noting that ℓ^a is Killing, this rate is a constant for geodesic observers. More generally, we parametrize it by

$$\lambda_o \equiv -(\sqrt{2}\mathcal{U}_o^a \ell_a)^{-1} > 0, \tag{26}$$

which coincides with the λ appearing in (17) if the motion is geodesic. Regardless of acceleration, a (not necessarily constant) λ_s can be defined analogously for the source, in which case proper times along $\mathcal{S}$ and $\mathcal{O}$ are related via

$$\frac{\mathrm{d}\tau_s}{\mathrm{d}\tau_o} = (\lambda_s/\lambda_o)\frac{\mathrm{d}u_s}{\mathrm{d}u_o}. \tag{27}$$

If both the source and the observer both move on geodesics, λ_s/λ_o is a constant and this equation is trivially integrated to obtain $\tau_s(\tau_o)$ in terms of $u_s(u_o)$.

3.2. Frequency shifts

The derivative $\mathrm{d}\tau_s/\mathrm{d}\tau_o$ appearing in (27) is directly observable. If a physical process on $\mathcal{S}$ occurs with a characteristic frequency ω_s—perhaps the frequency of a spectral line or the angular velocity of a pulsar—which is much larger than any frequencies associated with the gravitational wave or with the acceleration of $\mathcal{S}$, such a process would be observed on $\mathcal{O}$ to occur at frequency $\omega_o = (\mathrm{d}\tau_s/\mathrm{d}\tau_o)\omega_s$. This reduces to the familiar Doppler effect in flat spacetime, but more generally includes curvature corrections as well. One way to compute ω_o is to implicitly differentiate (23) and then substitute the result into (27). Alternatively, note that the gradient of Synge's function $\sigma(p_o, p_s)$ is tangent to the light ray which connects p_s to p_o. It is also parallel-transported along that ray, implying that

$$\frac{\omega_o}{\omega_s} = -\frac{\mathcal{U}_o^a \nabla_a \sigma}{\mathcal{U}_s^b \nabla_b \sigma} \tag{28}$$

in terms of the observer and source 4-velocities $\mathcal{U}_{o,s}^a$. The gradient in the numerator here is understood to be evaluated at p_o while the gradient in the denominator is understood to instead be evaluated at p_s. It follows from (28) that $\omega_o = \omega_s$ if $\mathcal{U}_o^a$ is equal to $\mathcal{U}_s^a$ parallel-transported along the relevant light ray, a generalization of the flat-spacetime result that the Doppler effect vanishes for comoving objects. Such a condition is physically unnatural, however, in curved spacetimes; the frequency shift is generically nonzero.

Equation (28) may be directly evaluated using (21) and (26). The result is conveniently expressed in terms of the 2-vectors

$$\boldsymbol{k}_o \equiv \frac{\langle\boldsymbol{\gamma}^{-1}\rangle^{-1}(\boldsymbol{x}_s - \boldsymbol{x}_{o\to s})}{\sqrt{2}\lambda_o(u_o - u_s)}, \qquad \boldsymbol{k}_s \equiv \frac{\langle\boldsymbol{\gamma}^{-1}\rangle^{-1}(\boldsymbol{x}_{s\to o} - \boldsymbol{x}_o)}{\sqrt{2}\lambda_s(u_o - u_s)}, \tag{29}$$

where

$$\boldsymbol{x}_{o \to s} \equiv \boldsymbol{x}_o - (u_o - u_s)\langle\boldsymbol{\gamma}^{-1}\rangle\boldsymbol{\gamma}(u_o)\dot{\boldsymbol{x}}_o, \quad \boldsymbol{x}_{s \to o} \equiv \boldsymbol{x}_s + (u_o - u_s)\langle\boldsymbol{\gamma}^{-1}\rangle\boldsymbol{\gamma}(u_s)\dot{\boldsymbol{x}}_s. \qquad (30)$$

All averages appearing here are to be evaluated between u_s and u_o, while, e.g., $\dot{\boldsymbol{x}}_o$ denotes a u-derivative of the observer's transverse coordinates evaluated at p_o. Up to overall factors included for later convenience, $\boldsymbol{k}_o$ and $\boldsymbol{k}_s$ are essentially transverse separations between the source and the observer evaluated either at the emission phase u_s or at the observation phase u_o. Causality does not allow any observation at $u = u_o$ to depend on properties of the source at that phase (except for special alignments where $u_s = u_o$), so the relevant observables instead involve an *extrapolation* of the source's position from $u = u_s$ to $u = u_o$ performed using the geodesic which is tangent to $\mathcal{S}$ at p_s. Comparing (16) and (30), $\boldsymbol{x}_{s \to o}$ represents precisely this kind of "osculating extrapolation." Similarly, $\boldsymbol{x}_{o \to s}$ extrapolates the transverse location of the observer from $u = u_o$ to $u = u_s$ using the geodesic tangent to $\mathcal{O}$ at p_o. In terms of $\boldsymbol{k}_o$ and $\boldsymbol{k}_s$, the frequency ratio in the presence of an arbitrary plane wave is

$$\frac{\omega_o}{\omega_s} = \frac{\mathrm{d}\tau_s}{\mathrm{d}\tau_o} = (\lambda_o/\lambda_s)\left(1 + \frac{\boldsymbol{\gamma}_{ij}^{-1}(u_s)k_s^i k_s^j - \boldsymbol{\gamma}_{ij}^{-1}(u_o)k_o^i k_o^j}{1 + \boldsymbol{\gamma}_{ij}^{-1}(u_o)k_o^i k_o^j}\right)^{-1}. \qquad (31)$$

This is valid for arbitrarily-moving sources and observers. It reduces in the flat limit $\gamma_{ij} \to \delta_{ij}$ to an expression for the ordinary Doppler shift. More generally, there is a sense in which the effects of relative motion and spacetime curvature can be disentangled by considering the time derivative of ω_o/ω_s [10, 11, 35].

Equation (31) simplifies significantly if the source and observer are assumed to move on geodesics which remain at fixed spatial coordinates. When this occurs, $\lambda_o = \lambda_s = 1$ and

$$\boldsymbol{k}_o = \boldsymbol{k}_s = \frac{\langle\boldsymbol{\gamma}^{-1}\rangle^{-1}(\boldsymbol{x}_s - \boldsymbol{x}_o)}{\sqrt{2}(u_o - u_s)}. \qquad (32)$$

The frequency shift then depends on the difference between inverse Rosen waveforms at the emission and observation events:

$$\frac{\omega_o - \omega_s}{\omega_o} = \frac{[\boldsymbol{\gamma}_{ij}^{-1}(u_o) - \boldsymbol{\gamma}_{ij}^{-1}(u_s)]k_o^i k_o^j}{1 + \boldsymbol{\gamma}_{kl}^{-1}(u_o)k_o^k k_o^l}. \qquad (33)$$

One deficiency with this formula is that k_o^i has no immediate physical interpretation. It is closely related, however, to the observed position of the source. As explained in Section 3.3, that position is naturally described in terms of the unit 3-vector $(\hat{\boldsymbol{k}}_\perp, \hat{k}_\parallel)$. Using (39) to relate this vector to $\boldsymbol{k}_o$, the frequency shift (33) can be rewritten as

$$\frac{\omega_o - \omega_s}{\omega_o} = \frac{1}{2}(1 + \cos\theta)^{-1}\hat{\boldsymbol{k}}_\perp^{\mathsf{T}}[\boldsymbol{I} - \boldsymbol{\xi}(u_o)\boldsymbol{\gamma}^{-1}(u_s)\boldsymbol{\xi}^{\mathsf{T}}(u_o)]\hat{\boldsymbol{k}}_\perp, \qquad (34)$$

where θ denotes the observed angle between the source and the gravitational wave propagation direction [cf. (41)]. Additionally, ξ_{ij} is a square root of γ_{ij} in the sense of (13). Although such roots are not unique, a particular choice must be made to in order to define an observer rest frame with respect to which the components of $\hat{\boldsymbol{k}}_\perp$ are defined. The ξ_{ij} appearing in (34) is the same as the one used in (38) to construct this frame.

Although exact, (34) is very similar to the first-order formula typically used when discussing gravitational wave measurements via pulsar timing [2, 14] or Doppler

velocimetry [36, 37, 38]. In terms of the first-order metric perturbation ϵh_{ij} which appears in (3), it is well-known that

$$\frac{\omega_o - \omega_s}{\omega_o} = \frac{\epsilon}{2}(1 + \cos\theta)^{-1}[h_{ij}(u_s) - h_{ij}(u_o)]\hat{k}_\perp^i \hat{k}_\perp^j + O(\epsilon^2). \qquad (35)$$

The physical meanings of the θ, $\hat{\boldsymbol{k}}_\perp$, and u_s which appear here are unchanged in the exact result, although their time-dependence is no longer trivial and relations to coordinate quantities are different. The metric difference $\epsilon[\boldsymbol{h}(u_s) - \boldsymbol{h}(u_o)]$ appearing in the first-order result is, however, generalized to

$$\boldsymbol{I} - \boldsymbol{\xi}(u_o)\boldsymbol{\gamma}^{-1}(u_s)\boldsymbol{\xi}^\mathsf{T}(u_o) = \boldsymbol{\xi}(u_o)[\boldsymbol{\gamma}^{-1}(u_o) - \boldsymbol{\gamma}^{-1}(u_s)]\boldsymbol{\xi}^\mathsf{T}(u_o). \qquad (36)$$

Approximations to (34) are discussed more fully in Section 4.2.3.

3.3. Source locations

Gravitational waves may affect not only a source's apparent spectrum, but also its location on the sky. Such locations could be described in terms of a 3-vector residing in the observer's instantaneous rest frame. More precisely, consider an orthonormal triad $(\boldsymbol{e}_\perp^a, e_\parallel^a)$ which is orthogonal to the observer's 4-velocity $\mathcal{U}_o^a$. It is convenient to align this triad such that one of its components is locked to the direction of propagation associated with the background plane wave. Projecting the null propagation direction ℓ^a into the observer's rest frame and normalizing, the longitudinal frame vector is then

$$e_\parallel^a \equiv \sqrt{2}\lambda_o(g^{ab} + \mathcal{U}_o^a\mathcal{U}_o^b)\ell_b = \sqrt{2}\lambda_o\ell^a - \mathcal{U}_o^a. \qquad (37)$$

It is also convenient to define the remaining two frame vectors by

$$\boldsymbol{e}_\perp^a \equiv \boldsymbol{\xi}^{-\mathsf{T}}(u_o)\left(\boldsymbol{\gamma}(u_o)\dot{\boldsymbol{x}}_o\frac{\partial}{\partial v} + \frac{\partial}{\partial \boldsymbol{x}}\right), \qquad (38)$$

where $\boldsymbol{\xi}$ is a particular matrix satisfying (13). It is easily verified that the resulting triad is indeed orthonormal and orthogonal to $\mathcal{U}_o^a$. It is also parallel-transported for geodesic observers. If $\mathcal{O}$ is not a geodesic, another frame—perhaps one which is Fermi-Walker transported—might be more natural. We nevertheless apply these definitions in all cases.

Recalling that the direction of the light ray connecting p_o to p_s is given by $-\nabla_a\sigma(p_o, p_s)$, its rest-frame components describe the observed location of $\mathcal{S}$. If the unit-normalized versions of these components are denoted by $(\hat{\boldsymbol{k}}_\perp^a, \hat{k}_\parallel^a)$, use of (21) results in

$$\hat{\boldsymbol{k}}_\perp = \frac{2\boldsymbol{\xi}^{-\mathsf{T}}(u_o)\boldsymbol{k}_o}{1 + \boldsymbol{k}_o^\mathsf{T}\boldsymbol{\gamma}^{-1}(u_o)\boldsymbol{k}_o}, \qquad \hat{k}_\parallel = \frac{1 - \boldsymbol{k}_o^\mathsf{T}\boldsymbol{\gamma}^{-1}(u_o)\boldsymbol{k}_o}{1 + \boldsymbol{k}_o^\mathsf{T}\boldsymbol{\gamma}^{-1}(u_o)\boldsymbol{k}_o}. \qquad (39)$$

By construction, $|\hat{\boldsymbol{k}}_\perp|^2 + \hat{k}_\parallel^2 = 1$. These expressions hold for arbitrarily-moving sources and observers in arbitrary plane wave spacetimes.

It is often sufficient to consider only the transverse 2-vector $\hat{\boldsymbol{k}}_\perp$. This is proportional to $\boldsymbol{\xi}^{-\mathsf{T}}(u_o)\boldsymbol{k}_o$, the first factor of which takes into account that the transverse 2-metric $\boldsymbol{\gamma}(u_o) = \boldsymbol{\xi}^\mathsf{T}(u_o)\boldsymbol{\xi}(u_o)$ is not Euclidean at the observer's location. The vector $\boldsymbol{k}_o$ is more interesting. Recalling its definition (29), the observer's transverse location $\boldsymbol{x}_o$ does not enter on its own, but instead appears via the osculating projection $\boldsymbol{x}_{o\to s}$. Objects therefore appear to be not where they "are," but where

they "would have been." This can be made more clear in terms of the distance measurements considered in Section 3.4. Using (42) and the area distance r_{area} (43),

$$\hat{\boldsymbol{k}}_{\perp} = \frac{1}{r_{\mathrm{area}}} \left(\frac{\det\langle\boldsymbol{\gamma}^{-1}\rangle}{\sqrt{\det\boldsymbol{\gamma}^{-1}(u_o)\boldsymbol{\gamma}^{-1}(u_s)}} \right)^{1/2} \boldsymbol{\xi}^{-\mathsf{T}}(u_o)\langle\boldsymbol{\gamma}^{-1}\rangle^{-1}(\boldsymbol{x}_s - \boldsymbol{x}_{o\to s}). \tag{40}$$

It is sometimes convenient to parametrize source locations by angles instead of vectors. Let (θ, ϕ) be polar coordinates constructed in the observer's sky such that θ corresponds to the apparent angle between the source and gravitational wave, while $\phi = 0$ coincides with the direction of $(\boldsymbol{e}_{\perp}^a)_1$. Then,

$$\hat{\boldsymbol{k}}_{\perp} = \left(\begin{array}{c} \cos\phi\sin\theta \\ \sin\phi\sin\theta \end{array} \right), \qquad \hat{k}_{\parallel} = \cos\theta. \tag{41}$$

Combining this with (39) shows that θ is explicitly

$$\tan^2(\theta/2) = \boldsymbol{k}_o^{\mathsf{T}}\boldsymbol{\gamma}^{-1}(u_o)\boldsymbol{k}_o. \tag{42}$$

One interesting characteristic of position measurements is that they can be used to deduce the presence of a gravitational wave even when observing very nearby sources. While knowledge of $\hat{\boldsymbol{k}}_{\perp}$ at any one instant isn't particularly meaningful, its time evolution is. This evolution can be nontrivial no matter how close $\mathcal{S}$ happens to be to $\mathcal{O}$. It is evident from the presence of $\boldsymbol{\gamma}^{-1}(u_o) - \boldsymbol{\gamma}^{-1}(u_s)$ in (33) that useful timing measurements are instead restricted to source-observer separations over which significant differences can be expected in the gravitational waveform.

3.4. Distances

The next observable we consider is the area distance r_{area}. If a source's angular size is resolvable and found to be equal to the small solid angle Ω in the observer's sky, there is a sense in which its physical area is $\Omega r_{\mathrm{area}}^2$ [12]. This is somewhat technical to derive, so we defer to the result obtained in [3] using Brinkmann coordinates. Translating that into Rosen coordinates while using (42) results in

$$r_{\mathrm{area}} = \frac{\sqrt{2}\lambda_o(u_o - u_s)}{1 + \cos\theta} \left(\frac{\det\langle\boldsymbol{\gamma}^{-1}\rangle}{\sqrt{\det\boldsymbol{\gamma}^{-1}(u_o)\boldsymbol{\gamma}^{-1}(u_s)}} \right)^{1/2}. \tag{43}$$

The first fraction here is essentially an affine distance to the source, while the second corrects this by taking into account the expansion of a thin bundle of light rays which converge on p_o. That latter correction is remarkably simple in terms of the Rosen waveform, depending only on the arithmetic and geometric averages of $\boldsymbol{\gamma}^{-1}$ between the source and the observer.

It can also be useful to describe a source in terms of its luminosity distance r_{lum}. This is related to the area distance via

$$r_{\mathrm{lum}} = \left(\frac{\mathrm{d}\tau_s}{\mathrm{d}\tau_o} \right)^{-2} r_{\mathrm{area}}. \tag{44}$$

One factor of $\mathrm{d}\tau_s/\mathrm{d}\tau_o$ occurs due to the frequency shift experienced by light traveling from $\mathcal{S}$ to $\mathcal{O}$, while the second arises from considering bundles of light rays which converge on p_s rather than p_o. An explicit formula for the luminosity distance follows immediately by substituting (31) and (43) into (44).

4. Perturbation theory

Equations (23), (31), (40), (43), and (44) provide exact prescriptions for the time delays, frequency shifts, positions, and distances of generic sources in plane wave spacetimes. We now consider their perturbative expansions. This done for three reasons: First, it provides a clear connection between the exact results derived here and approximations which have appeared in literature. Second, some physical implications of the optical formulae are more easily understand when written in an approximate form. Finally, the results of Section 3 can be expanded beyond the lowest-order approximation which has typically been considered in the past. Doing so, we demonstrate that some higher-order corrections grow very rapidly with the source-observer distance, and can sometimes be significant even for gravitational waves with very small strain amplitudes.

There are two types of nonlinearity which arise here. The first of these has its origin in the nonlinearity of Einstein's equation as applied to the Rosen-type plane wave metric (12). Perturbative expansions of this waveform are considered in Section 4.1, and are sufficient to qualitatively understand that nonlinear effects can accumulate at large distances. The various gravitational wave observables are, however, nonlinear functionals of γ_{ij}. This is taken into account when deriving explicit second-order expansions for various observables in Section 4.2. Example applications are finally discussed in Section 5.

4.1. Expanding the metric

As explained in Section 2.2, gravitational plane waves in general relativity can be trivially described in terms of the Brinkmann waveform H_{ij}. This directly determines the curvature, and is restricted by the vacuum Einstein equation only to be trace-free. The observables discussed in Section 3 are not, however, written in terms of H_{ij}. They instead depend on the Rosen waveform γ_{ij}, which is related via the nonlinear and nonlocal expressions (11) and (13). Although the vacuum Einstein equation could be applied to find a nonlinear differential equation for the Rosen waveform alone, we take the perspective that it is more natural to instead describe a plane wave in terms of H_{ij} and then to derive γ_{ij} from that. It is also convenient to view the perturbative expansion performed here not as an approximation for a single system which involves a small quantity ϵ, but rather as an approximation for an entire *family* of systems which are smoothly parametrized by ϵ. Orders in perturbation theory then correspond to differentiations with respect to ϵ evaluated at $\epsilon = 0$.

The precise family of plane wave spacetimes considered here‖ is defined to be the set of Brinkmann line elements (6) with

$$H_{ij}(u; \epsilon) = \epsilon \mathfrak{H}_{ij}(u), \qquad \epsilon \geq 0. \tag{45}$$

The "reference waveform" $\mathfrak{H}_{ij}(u) = \partial_\epsilon H_{ij}(u; \epsilon)$ is assumed to be known and independent of ϵ. Additionally supposing that $\operatorname{tr} \mathfrak{H}(u) = 0$, it follows from (7) that each spacetime in this family is an exact solution to the vacuum Einstein equation. The parameter ϵ controls the amplitude of a wave's curvature, but not its polarization,

‖ It can sometimes be interesting to instead consider families of waves where the curvature depends smoothly on ϵ, *u and* u/ϵ. Any portions involving u/ϵ vary rapidly as $\epsilon \to 0$, thus evoking the concept of a "high-frequency limit" [39, 40]. Considering such families is equivalent to a type a singular perturbation theory [as opposed to the regular perturbation associated with (45)]. See also the last paragraph of Section 4.1.2.

frequency, or anything else. As expected from such an interpretation, different members of this family are physically distinct: Choosing any nonzero ϵ and any $\epsilon' \neq \epsilon$, the waveform $H_{ij}(u; \epsilon') = (\epsilon'/\epsilon) H_{ij}(u; \epsilon)$ cannot be transformed into $H_{ij}(u; \epsilon)$ using the gauge transformation (9). It is also clear that the wave disappears entirely entirely in the $\epsilon \to 0$ limit.

Given a trace-free $\mathfrak{H}_{ij}(u)$, an associated Rosen waveform $\gamma_{ij}(u; \epsilon)$ may be found by first constructing a matrix $\xi_{ij}(u; \epsilon)$ with the expansion

$$\boldsymbol{\xi}(u; \epsilon) = \boldsymbol{\xi}_{(0)}(u) + \ldots + \epsilon^n \boldsymbol{\xi}_{(n)}(u) + \ldots. \tag{46}$$

Applying (11),

$$\ddot{\boldsymbol{\xi}}_{(0)} = 0, \qquad \ddot{\boldsymbol{\xi}}_{(n)} = \mathfrak{H} \boldsymbol{\xi}_{(n-1)} \tag{47}$$

for all $n \geq 1$. Iteratively solving these equations results in an approximation for $\xi_{ij}(u; \epsilon)$. Using it together with (13) produces a Rosen waveform $\gamma_{ij}(u; \epsilon)$ with the expansion coefficients

$$\boldsymbol{\gamma}_{(n)}(u) \equiv \frac{1}{n!} \partial_\epsilon^n \boldsymbol{\gamma}(u; \epsilon)|_{\epsilon=0} = \sum_{p+q=n} \boldsymbol{\xi}_{(p)}^{\mathsf{T}}(u) \boldsymbol{\xi}_{(q)}(u). \tag{48}$$

In many cases, we use the more standard notation $\boldsymbol{h}(u)$ for the first-order perturbation $\boldsymbol{\gamma}_{(1)}(u)$ [see (3)].

As already emphasized in Section 2.3, different Rosen waveforms—corresponding to different initial conditions for (11)—can be used to describe the same physics. Ambiguities of this kind are easily resolved for the sandwich waves described in Section 2.4, in which case it is natural to fix a particular waveform by demanding that $\gamma_{ij} = \xi_{ij} = \delta_{ij}$ in one of the locally-flat regions. More generally, however, there does not appear to be any "preferred" choice.

Our approach is to fix a particular solution for ξ_{ij}, and then to note that all other possibilities are related via (19). Let this particular solution satisfy the non-perturbative initial condition

$$\xi_{ij}(u_0; \epsilon) = \delta_{ij}, \qquad \dot{\xi}_{ij}(u_0; \epsilon) = 0 \tag{49}$$

for some constant u_0. It then follows from (47) that $\boldsymbol{\xi}_{(0)} = \boldsymbol{I}$ and

$$\boldsymbol{\xi}_{(n)}(u) = \int_{u_0}^u \mathrm{d}u_1 \int_{u_0}^{u_1} \mathrm{d}u_2 \mathfrak{H}(u_2) \boldsymbol{\xi}_{(n-1)}(u_2) \tag{50}$$

and for all $n \geq 1$. Hence,

$$\operatorname{tr} \boldsymbol{\xi}_{(n)} = \boldsymbol{\xi}_{(n)}^{\mathsf{T}} - \boldsymbol{\xi}_{(n)} = 0 \qquad (n \text{ odd}), \tag{51}$$

and

$$\boldsymbol{\xi}_{(n)} + \boldsymbol{\xi}_{(n)}^{\mathsf{T}} = (\operatorname{tr} \boldsymbol{\xi}_{(n)}) \boldsymbol{I} \qquad (n \text{ even}). \tag{52}$$

Combining these constraints with (48) shows that each $\boldsymbol{\gamma}_{(n)}$ generated by a $\boldsymbol{\xi}$ which satisfies (49) is symmetric and that

$$\operatorname{tr} \boldsymbol{\gamma}_{(n)} = 0 \quad (n \text{ odd}), \qquad \boldsymbol{\gamma}_{(n)} = \frac{1}{2} (\operatorname{tr} \boldsymbol{\gamma}_{(n)}) \boldsymbol{I} \quad (n \text{ even}). \tag{53}$$

The familiar tracelessness of the first-order TT-gauge perturbation $\boldsymbol{h} = \boldsymbol{\gamma}_{(1)}$ therefore generalizes to all odd-order metric perturbations. It does not generalize to even orders; those expansion coefficients are instead "pure trace."

Through second order, these results imply that the particular Rosen waveform defined by (49) is explicitly

$$\boldsymbol{\gamma}(u;\epsilon) = \boldsymbol{I} + 2\epsilon \int_{u_0}^u \mathrm{d}u_1 \int_{u_0}^{u_1} \mathrm{d}u_2 \, \mathfrak{H}(u_2) + \epsilon^2 \operatorname{tr}\left[\frac{1}{2}\left(\int_{u_0}^u \mathrm{d}u_1 \int_{u_0}^{u_1} \mathrm{d}u_2 \, \mathfrak{H}(u_2)\right)^2\right.$$
$$\left. + \int_{u_0}^u \mathrm{d}u_1 \int_{u_0}^{u_1} \mathrm{d}u_2 \int_{u_0}^{u_2} \mathrm{d}u_3 \int_{u_0}^{u_3} \mathrm{d}u_4 \, \mathfrak{H}(u_2)\mathfrak{H}(u_4)\right] \boldsymbol{I} + O(\epsilon^3). \tag{54}$$

The amplitude of the second line here generically grows with u. This can be seen more clearly if the waveform is rewritten in terms of the first-order perturbation h_{ij} instead of $\mathfrak{H}_{ij} = \frac{1}{2}\ddot{h}_{ij}$. Integrating by parts,

$$\boldsymbol{\gamma}(u;\epsilon) = \boldsymbol{I} + \epsilon \boldsymbol{h}(u) + \frac{1}{4}\epsilon^2 \operatorname{tr}\left[\boldsymbol{h}^2(u) - \int_{u_0}^u \mathrm{d}u_1 \int_{u_0}^{u_1} \mathrm{d}u_2 \, \dot{\boldsymbol{h}}^2(u_2)\right] \boldsymbol{I} + O(\epsilon^3). \tag{55}$$

The trace of $\dot{\boldsymbol{h}}^2$ cannot be negative, implying that the second-order metric perturbation typically grows with u. Indeed, there exists an ϵ-dependent scale beyond which the second-order term outpaces the first. We now consider two examples which demonstrate this explicitly.

4.1.1. Gravitational wave bursts with memory Consider a sandwich wave as described in Section 2.4. More specifically, consider an ϵ-dependent family of waves (45) with $\mathfrak{H}_{ij}(u)$ zero everywhere except in a small region $u \in (-\delta, 0)$ inside of which the curvature oscillates several times. Choosing $u_0 < -\delta$ in (49) guarantees that the metric before the burst is trivial: $\gamma_{ij}(u;\epsilon) = \delta_{ij}$. The metric after the burst must instead be generated by the square of (20), where $\boldsymbol{a}_{\mathcal{F}_+}(\epsilon)$ and $\boldsymbol{b}_{\mathcal{F}_+}(\epsilon)$ are constant matrices determined by the details of the curved region. If $\boldsymbol{a}_{\mathcal{F}_+}(\epsilon) \neq \boldsymbol{I}$ or $\boldsymbol{b}_{\mathcal{F}_+}(\epsilon) \neq 0$, the gravitational wave burst is said to exhibit "memory" [41, 42] in the sense that it permanently displaces initially-stationary pairs of freely-falling test particles. It follows from (50) that the first and second-order perturbations are

$$(\boldsymbol{a}_{\mathcal{F}_+})_{(1)} = \frac{1}{2}\boldsymbol{h}(0) = \int_{-\delta}^0 \mathrm{d}u_1 \int_{-\delta}^{u_1} \mathrm{d}u_2 \, \mathfrak{H}(u_2), \tag{56}$$

$$(\boldsymbol{b}_{\mathcal{F}_+})_{(1)} = \frac{1}{2}\dot{\boldsymbol{h}}(0) = \int_{-\delta}^0 \mathrm{d}u_1 \, \mathfrak{H}(u_1), \tag{57}$$

and

$$(\boldsymbol{a}_{\mathcal{F}_+})_{(2)} = \frac{1}{4}\operatorname{tr}\left[(\boldsymbol{a}_{\mathcal{F}_+})_{(1)}^2 - \frac{1}{2}\int_{-\delta}^0 \mathrm{d}u_1 \int_{-\delta}^{u_1} \mathrm{d}u_2 \, \dot{\boldsymbol{h}}^2(u_2)\right] \boldsymbol{I}, \tag{58}$$

$$(\boldsymbol{b}_{\mathcal{F}_+})_{(2)} = \frac{1}{2}\operatorname{tr}\left[(\boldsymbol{a}_{\mathcal{F}_+})_{(1)}(\boldsymbol{b}_{\mathcal{F}_+})_{(1)} - \frac{1}{4}\int_{-\delta}^0 \mathrm{d}u_1 \, \dot{\boldsymbol{h}}^2(u_1)\right] \boldsymbol{I}. \tag{59}$$

Although gravitational wave bursts with memory can arise from many physical scenarios, classic discussions [42, 43] consider those waves which are emitted either from the scattering of multiple masses or the explosion of one mass into multiple unbound components. For cases like these, the quadrupole formula suggests that $(\boldsymbol{b}_{\mathcal{F}_+})_{(1)} = 0$.¶ Assuming this, a coordinate rotation may always be performed

---

¶ The condition $(\boldsymbol{b}_{\mathcal{F}_+})_{(1)} = 0$ implies that pairs of test particles which are comoving before the burst are also comoving after the burst; only their displacements might be permanently affected at $O(\epsilon)$. Some cases where an additional "velocity memory" arises are discussed in [44]. See also [43, 45] for an electromagnetic memory effect where nontrivial velocity changes occur even in simple scattering problems.

together with a rescaling of ϵ such that

$$(\boldsymbol{a}_{\mathcal{F}_+})_{(1)} = \frac{1}{2} \begin{pmatrix} 1 & 0 \\ 0 & -1 \end{pmatrix}. \tag{60}$$

Now consider second order effects. It follows from (59) that even though $\boldsymbol{b}_{\mathcal{F}_+}$ vanishes at first order, it *cannot* vanish at second order. Indeed, $\mathrm{tr}(\boldsymbol{b}_{\mathcal{F}_+})_{(2)} < 0$. Applying (13) and (20), the second-order waveform is explicitly

$$\boldsymbol{\gamma}(u; \epsilon) = \boldsymbol{I} + \epsilon \left\{ \begin{pmatrix} 1 & 0 \\ 0 & -1 \end{pmatrix} + \frac{1}{4}\epsilon \left[1 + 4\,\mathrm{tr}(\boldsymbol{a}_{\mathcal{F}_+})_{(2)} \right] \boldsymbol{I} \right\}$$
$$+ \epsilon^2 u \left[\mathrm{tr}(\boldsymbol{b}_{\mathcal{F}_+})_{(2)} \right] \boldsymbol{I} + O(\epsilon^3) \tag{61}$$

when $u_o > 0$. If the first-order waveform inside a burst is schematically of the form $h(u) \sim \cos \omega u$ and oscillates $N \sim \omega\delta$ times, it follows from (59) that $\mathrm{tr}(\boldsymbol{b}_{\mathcal{F}_+})_{(2)} \sim -N\omega$. The second-order term here therefore becomes comparable to the first-order terms when

$$\omega u \sim (\epsilon N)^{-1} \gg 1. \tag{62}$$

Of course, $\boldsymbol{\gamma}_{(1)}$ and $\boldsymbol{\gamma}_{(2)}$ are qualitatively different when this occurs. One is trace-free while the the other is a pure trace. On even larger scales where $\omega u \sim (\epsilon^2 N)^{-1}$, the determinant of the Rosen waveform goes to zero. Recalling the line element (12), the metric itself becomes singular on this scale. Such effects are not an artifact of the perturbative expansion, but instead signal the breakdown of the Rosen coordinate system.

4.1.2. Monochromatic waves Another instructive example is provided by a linearly-polarized gravitational wave which is monochromatic with angular frequency ω in the sense that it can be described by the family (45) with

$$\mathfrak{H}(u) = \frac{\omega^2}{2} \begin{pmatrix} 1 & 0 \\ 0 & -1 \end{pmatrix} \cos \omega u. \tag{63}$$

If $\omega = 1$, the $2, 2$-component of $\xi_{ij}(u; \epsilon)$ satisfies the Mathieu equation (1). We now show that important features of the higher-order metric perturbation associated with a monochromatic gravitational wave are captured by the approximate solution (2) to that equation.

Although it is possible to express all components of $\gamma_{ij}(u; \epsilon)$ exactly in terms of Mathieu functions, consider instead the perturbative expansion described above. This first requires imposing initial conditions for $\xi_{ij}(u; \epsilon)$. Unfortunately, there is no natural phase at which to apply (49). Indeed, all choices are more complicated than necessary. Setting $u_0 = 0$ for definiteness, (48) and (50) imply that h_{ij} involves an oscillating term as well as a constant offset. Eliminating this offset by modifying the initial condition at $O(\epsilon)$ recovers the expected

$$\boldsymbol{h}(u) = - \begin{pmatrix} 1 & 0 \\ 0 & -1 \end{pmatrix} \cos \omega u. \tag{64}$$

The second-order perturbation is then

$$\boldsymbol{\gamma}_{(2)}(u) = \frac{1}{16} [1 - 2(\omega u)^2 + 3\cos 2\omega u] \boldsymbol{I} + 2[\boldsymbol{\xi}_{(2)}(0) + u\dot{\boldsymbol{\xi}}_{(2)}(0)], \tag{65}$$

where the final two terms allow for $O(\epsilon^2)$ modifications to the initial condition (49). It is clear, however, that no matter what these modifications are, the term proportional to
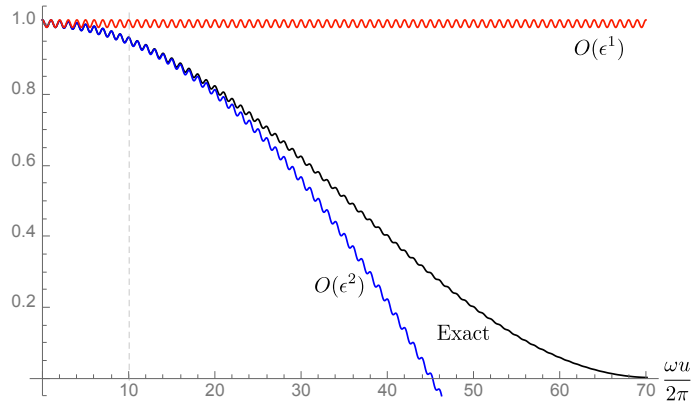
Figure 2: Plot of $\gamma_{22}(u)$ for a monochromatic gravitational wave with $\mathfrak{H}_{ij}(u)$ given by (63) and $\epsilon = 0.01$. An exact solution is shown together with its first and second-order approximations. Initial conditions for all three curves are matched at $u = 0$. The $O(\epsilon)$ approximation is poor after $\epsilon^{-1/2} = 10$ curvature oscillations, although the $O(\epsilon^2)$ approximation still works well there. A coordinate singularity appears in fewer than $\epsilon^{-1} = 100$ oscillations.

u^2 cannot be eliminated. It is a second-order perturbation which becomes comparable to the first-order perturbation when

$$\omega u \sim \epsilon^{-1/2} \gg 1. \tag{66}$$

This can be understood intuitively as a version of (62) where the number of gravitational wave oscillations N isn't fixed, but is instead of order ωu. For a given wave amplitude ϵ, it follows that nonlinear effects tend to be more important for approximately-monochromatic waves than for bursts. Also note that as suggested by (65), Rosen coordinates break down when $\omega u \sim \epsilon^{-1} \gg \epsilon^{-1/2}$. This is illustrated explicitly in Figure 2 for the case $\epsilon = 0.01$.

The large nonlinear effects considered thus far do not oscillate. Monochromatic waves where $\epsilon \ll 1$ first experience relatively-large oscillatory corrections at $O(\epsilon^3)$. Assuming initial conditions for $\boldsymbol{\xi}_{(1)}$ such that (64) holds, the large-u portions of $\boldsymbol{\gamma}_{(2)}$ and $\boldsymbol{\gamma}_{(3)}$ can be viewed as conformal corrections to the first-order waveform:

$$\boldsymbol{\gamma}(u; \epsilon) = \left[1 - \frac{1}{8} (\epsilon \omega u)^2 \right] \left[\boldsymbol{I} - \epsilon \begin{pmatrix} 1 & 0 \\ 0 & -1 \end{pmatrix} \cos \omega u \right] + \ldots + O(\epsilon^4). \tag{67}$$

The ellipses here denote omitted terms at second and third order which grow more slowly than u^2.

The growing nonlinearities we discuss can in some ways be interpreted as manifestations of an averaging effect which occurs more explicitly when considering "high-frequency" perturbations where $H_{ij}(u; \epsilon)$ smoothly depends on ϵ. In that context, the zeroth-order metric is no longer Minkowski, but instead satisfies the non-vacuum Einstein equation with an effective stress-energy tensor sourced by the gravitational wave [39, 40]. Indeed, this stress-energy tensor is controlled by an average of the same "energy density" $\dot{\boldsymbol{h}}^2$ which is responsible for the second-order metric (55) in an ordinary perturbative expansion. The high-frequency viewpoint is not pursued here for several reasons. First, its formulation requires choosing one small parameter

which simultaneously controls both wave amplitudes and distances. This somewhat limits its flexibility and clarity for the questions considered here. More importantly, different observables can react very differently when considering non-smooth families of spacetimes. The usual high-frequency formulations in general relativity are designed to compute metrics which are limits of solutions to Einstein's equation. It is not necessarily true, however, that limits of optical observables can be easily described in terms of these same metrics (or even that limits exist at all).

4.2. Gravitational wave observables

Perturbative expansions for the various observables computed in Section 3 may now be found for families of plane waves described by (45). Completely general expressions would be quite complicated, so we restrict attention only to those cases where the observer $\mathcal{O}$ remains fixed at the spatial coordinates $(\boldsymbol{x}_o, z_o)$. Also suppose that the source $\mathcal{S}$ remains fixed at $(\boldsymbol{x}_s, z_s)$. As guaranteed by the construction of the Rosen coordinate system described in Section 2.3, all such worldlines are timelike geodesics. They are not preserved, however, by changes in the Rosen waveform; coordinate transformations (19) which modify γ_{ij} also impart initially-stationary geodesics with nonzero coordinate velocities. Our assumption that sources and observers remain at fixed spatial coordinates is therefore coupled to the choice of a particular Rosen waveform. Although no detailed prescription is used here, we do assume that

$$\boldsymbol{\xi}_{(0)} = \boldsymbol{\gamma}_{(0)} = \boldsymbol{I}, \qquad \boldsymbol{\xi}_{(1)} = \boldsymbol{\xi}_{(1)}^{\mathsf{T}} = \frac{1}{2}\boldsymbol{\gamma}_{(1)}, \qquad \operatorname{tr}\boldsymbol{\gamma}_{(1)} = 0, \qquad \boldsymbol{\gamma}_{(2)} \propto \boldsymbol{I}. \tag{68}$$

These equations are implied by the initial condition (49), although they also hold more generally.

4.2.1. Zeroth order
Our first step is to compute all observables in the flat-spacetime limit $\epsilon \to 0$. Denoting orders in perturbation theory by analogy with (46), the zeroth-order observables are

$$r_{\text{area}}^{(0)} = r_{\text{lum}}^{(0)} = r \equiv \sqrt{|\boldsymbol{x}_s - \boldsymbol{x}_o|^2 + (z_s - z_o)^2}, \tag{69}$$

$$\omega_o^{(0)} - \omega_s = 0, \tag{70}$$

$$\hat{\boldsymbol{k}}_\perp^{(0)} = (\boldsymbol{x}_s - \boldsymbol{x}_o)/r, \tag{71}$$

$$\cos\theta_{(0)} = (z_s - z_o)/r. \tag{72}$$

As expected, both the area and luminosity distances reduce to the coordinate distance r at this order. Frequency shifts also vanish, and a source's apparent location in the observer's sky is given by the expected function of its coordinate position. Somewhat less obviously, (23) implies that the zeroth-order emission phase $u_s^{(0)}$ is

$$u_s^{(0)} = u_o - \frac{r}{\sqrt{2}}(1 + \cos\theta_{(0)}) \tag{73}$$

in terms of the observation phase u_o.

All higher-order perturbative expressions obtained below depend in various ways on these zeroth-order quantities. Consistently retaining "(0)" subscripts or superscripts on each of them would considerably increase clutter, so this notation is suppressed when no confusion should arise.

4.2.2. Time of flight Differentiating (23) with respect to ϵ, the presence of a nontrivial gravitational wave alters the emission phase (73) via the first-order perturbation

$$\frac{u_s^{(1)}}{r} = -\frac{1}{2\sqrt{2}}\langle h_{ij}\rangle \hat{k}_\perp^i \hat{k}_\perp^j. \tag{74}$$

The $\hat{\boldsymbol{k}}_\perp$ appearing here is understood to refer to the zeroth-order direction $\hat{\boldsymbol{k}}_\perp^{(0)}$. Similarly, $\langle h_{ij}\rangle$ denotes an average between $u_s^{(0)}$ and u_o. Decomposing h_{ij} into its $+$ and $\times$ components via (4), the emission phase perturbation can alternatively be written as

$$\frac{u_s^{(1)}}{r} = -\frac{1}{2\sqrt{2}}\left[\langle h_+\rangle \cos 2\phi + \langle h_\times\rangle \sin 2\phi\right]\sin^2\theta. \tag{75}$$

This vanishes for all sources which are aligned ($\theta_{(0)} = 0$) or anti-aligned ($\theta_{(0)} = \pi$) with the gravitational wave. If that wave is linearly-polarized, coordinates may be chosen such that $h_\times = 0$, implying that $u_s^{(1)}$ also vanishes for any source which is nominally located on one of the four meridians

$$\phi_{(0)} = (1 + 2n)\pi/4, \qquad n = 0, 1, 2, 3. \tag{76}$$

Regardless of polarization, the averages appearing in (75) are typically small if the waveform is approximately oscillatory and there are many oscillations between the source and the observer. These averages can be important, however, when there is significant gravitational memory.

The second-order perturbation to u_s is more complicated. Differentiating (23) twice with respect to ϵ,

$$\begin{aligned}\frac{u_s^{(2)}}{r} = & -\frac{1}{4\sqrt{2}}\operatorname{tr}\left[\langle\boldsymbol{\gamma}_{(2)}\rangle + \langle\boldsymbol{h}\rangle^2 - \langle\boldsymbol{h}^2\rangle\right]\sin^2\theta \\ & + \frac{u_s^{(1)}}{2r}\left(\frac{h_{ij}(u_s) - \langle h_{ij}\rangle}{1 + \cos\theta} - \frac{1}{2}\langle h_{ij}\rangle\right)\hat{k}_\perp^i \hat{k}_\perp^j.\end{aligned} \tag{77}$$

Unlike its first-order analog, $u_s^{(2)}$ does not tend to zero for oscillatory, memory-free waves at large distances. Part of it is also independent of $\phi_{(0)}$.

4.2.3. Frequency shifts Expanding (34) through first order in ϵ shows that

$$\frac{\omega_o^{(1)}}{\omega_s} = \frac{1}{2}(1 + \cos\theta)^{-1}[h_{ij}(u_s) - h_{ij}(u_o)]\hat{k}_\perp^i \hat{k}_\perp^j. \tag{78}$$

Combining this with (70) immediately reproduces the well-known [2, 14] first-order approximation (35) for the frequency shift induced by a gravitational wave. In terms of h_+ and $h_\times$, it is more explicitly

$$\frac{\omega_o^{(1)}}{\omega_s} = \frac{1}{2}(1 - \cos\theta)\left\{[h_+(u_s) - h_+(u_o)]\cos 2\phi + [h_\times(u_s) - h_\times(u_o)]\sin 2\phi\right\}. \tag{79}$$

Equation (73) implies that $u_s^{(0)} \to u_o$ as $\theta_{(0)} \to \pi$, so $\omega_o^{(1)} = 0$ for any sources which are aligned or anti-aligned with the background gravitational wave. If the wave is linearly-polarized and coordinates are chosen such that $h_\times = 0$, first-order frequency shifts also vanish when $\phi_{(0)}$ satisfies (76).

Regardless of polarization, expanding (34) through second order in ϵ results in the additional correction

$$\frac{\omega_o^{(2)}}{\omega_s} = \frac{1}{4}(1 - \cos\theta)\,\mathrm{tr}\left\{\boldsymbol{\gamma}_{(2)}(u_s) - \boldsymbol{\gamma}_{(2)}(u_o) + [\boldsymbol{h}(u_s) - \boldsymbol{h}(u_o)][2\langle\boldsymbol{h}\rangle - \boldsymbol{h}(u_s) - \boldsymbol{h}(u_o)]\right\}$$
$$+ \frac{1}{2}(1 + \cos\theta)^{-1}\left[(\omega_o^{(1)}/\omega_s)[h_{ij}(u_s) - (3 + \cos\theta)\langle h_{ij}\rangle] + u_s^{(1)}\dot{h}_{ij}(u_s)\right]\hat{k}_\perp^i\hat{k}_\perp^j. \quad (80)$$

This too vanishes when $\theta_{(0)} \to 0$ or $\theta_{(0)} \to \pi$. The difference $\boldsymbol{\gamma}_{(2)}(u_s^{(0)}) - \boldsymbol{\gamma}_{(2)}(u_o)$ which appears here is directly analogous to the $\boldsymbol{h}(u_s^{(0)}) - \boldsymbol{h}(u_o)$ arising in $\omega_o^{(1)}/\omega_s$. The final term involving $\dot{\boldsymbol{h}}(u_s)$ may also be interpreted as a straightforward correction to the first-order expression obtained by the replacement $\boldsymbol{h}(u_s^{(0)}) \to \boldsymbol{h}(u_s^{(0)} + \epsilon u_s^{(1)} + \ldots)$.

4.2.4. Source locations The apparent location of a source is governed via (41) by the unit vector $(\hat{\boldsymbol{k}}_\perp, \hat{k}_\parallel)$ introduced in Section 3.3. Differentiating (39) once with respect to ϵ shows that the first-order astrometric effects of a gravitational plane wave follow from

$$\hat{\boldsymbol{k}}_\perp^{(1)} = \left[\langle\boldsymbol{h}\rangle - \frac{1}{2}\boldsymbol{h}(u_o)\right]\hat{\boldsymbol{k}}_\perp + \frac{1}{2}\left[\left(\frac{h_{ij}(u_o) - \langle h_{ij}\rangle}{1 + \cos\theta} - \langle h_{ij}\rangle\right)\hat{k}_\perp^i\hat{k}_\perp^j\right]\hat{\boldsymbol{k}}_\perp, \quad (81)$$

a result which has also been derived (using different methods) in [4]. One of its consequences is that the angle θ between the source and the gravitational wave is perturbed by

$$\theta_{(1)} = \frac{1}{2}\left\{\left[\langle h_{ij}\rangle - h_{ij}(u_o)\right] + \langle h_{ij}\rangle\cos\theta\right\}\hat{k}_\perp^i\hat{k}_\perp^j\csc\theta. \quad (82)$$

If a gravitational wave is linearly-polarized with $h_\times = 0$, sources which nominally lie on the meridians (76) experience vanishing latitudinal motion. These sources can, however, appear to rotate slightly around the gravitational wave propagation direction: $\theta_{(1)} = 0$ but $\phi_{(1)} = \pm[\langle h_+\rangle - \frac{1}{2}h_+(u_o)]$.

Regardless of polarization, two special cases of (81) may be understood immediately. The first of these supposes that $\langle h_{ij}\rangle$ can be neglected, and may be thought of as a "large-r" limit in the presence of memory-free waves:

$$\hat{\boldsymbol{k}}_\perp^{(1)} \to \frac{1}{2}\left\{(1 - \cos\theta)\left[h_+(u_o)\cos 2\phi + h_\times(u_o)\sin 2\phi\right]\boldsymbol{I} - \boldsymbol{h}(u_o)\right\}\hat{\boldsymbol{k}}_\perp. \quad (83)$$

Gravitational waves can also produce nontrivial astrometric effects in a "small-r" limit where $\langle h_{ij}\rangle \to h_{ij}(u_o)$ and

$$\hat{\boldsymbol{k}}_\perp^{(1)} \to \frac{1}{2}\left\{\boldsymbol{h}(u_o) - \sin^2\theta\left[h_+(u_o)\cos 2\phi + h_\times(u_o)\sin 2\phi\right]\boldsymbol{I}\right\}\hat{\boldsymbol{k}}_\perp. \quad (84)$$

In either of these cases, first-order position perturbations depend on the waveform only at $u = u_o$. The angular dependence of this effect is nevertheless distinct for near and distant sources.

If a gravitational wave is linearly-polarized, the matrices which multiply $\hat{\boldsymbol{k}}_\perp^{(0)}$ in (83) and (84) depend on u_o only via an overall scaling. Objects in both limits therefore appear to move coherently along straight lines in the presence of linearly-polarized gravitational waves. The orientations and relative lengths of these lines depend on a particular source's nominal location $(\theta_{(0)}, \phi_{(0)})$ in the observer's sky. Apparent motions which are not rectilinear can be induced in either the small-r or large-r limits by gravitational waves which are not linearly-polarized. Such motions can also arise

from linearly-polarized waves when $\langle h_{ij} \rangle$ is neither negligible nor approximately equal to $h_{ij}(u_o)$.

Astrometric effects are significantly more complicated at higher orders. We therefore present second-order corrections only for θ. Differentiating (42) twice with respect to ϵ shows that

$$
\begin{aligned}
\theta_{(2)} = \frac{1}{4} \operatorname{tr} \Bigg\{ & \left[\langle \boldsymbol{\gamma}_{(2)} \rangle - \boldsymbol{\gamma}_{(2)}(u_o) \right] + \langle \boldsymbol{\gamma}_{(2)} \rangle \cos\theta + (1 + \cos\theta) \left[\langle \boldsymbol{h} \rangle^2 - \langle \boldsymbol{h}^2 \rangle \right] \\
& + [\langle \boldsymbol{h} \rangle - \boldsymbol{h}(u_o)]^2 \Bigg\} \sin\theta + \left\{ \frac{u_s^{(1)}}{\sqrt{2}r} \left[\frac{\langle h_{ij} \rangle - 2h_{ij}(u_o)}{1 + \cos\theta} + \frac{1}{2}(4 + \cos\theta)\langle h_{ij} \rangle \right. \right. \\
& \left. - h_{ij}(u_s) \right] \hat{k}_\perp^i \hat{k}_\perp^j - \frac{1}{2}(2 - \cos\theta)\theta_{(1)}^2 \Bigg\} \csc\theta.
\end{aligned} \tag{85}
$$

All terms involving $\boldsymbol{\gamma}_{(2)}$ in this equation are direct generalizations of the first-order metric perturbations appearing in $\theta_{(1)}$.

4.2.5. Distances The last observables we consider are the area distance r_{area} and the luminosity distance r_{lum}. It follows from (43) and (44) that their first-order perturbations are

$$
\frac{r_{\text{area}}^{(1)}}{r} = \frac{1}{2} \left(\langle h_{ij} \rangle + \frac{\langle h_{ij} \rangle - h_{ij}(u_o)}{1 + \cos\theta} \right) \hat{k}_\perp^i \hat{k}_\perp^j, \tag{86}
$$

and

$$
\frac{r_{\text{lum}}^{(1)}}{r} = \frac{r_{\text{area}}^{(1)}}{r} + (1 + \cos\theta)^{-1} [h_{ij}(u_o) - h_{ij}(u_s)] \hat{k}_\perp^i \hat{k}_\perp^j. \tag{87}
$$

The second of these expressions describes how an object's apparent brightness is affected by a gravitational wave. It has sometimes been stated in the literature that gravity first affects brightnesses only at second order in general relativity (e.g., [5, 46]). A typical argument appeals to the Raychaudhuri equation, which can be used to show that the expansion of a null congruence is unperturbed through first order *for objects at a fixed affine distance*. This is misleading, however. Gravitational waves (and more general spacetimes) do affect affine distances at $O(\epsilon)$. This and the first-order time dilation both contribute nontrivial first-order perturbations to r_{area} and r_{lum}.

Second-order distance perturbations must take into account changes in a source's affine distance, time dilation, and, unlike in the first-order case, the gravitational focusing of null congruences. All of these effects are taken into account automatically by differentiating (43) twice with respect to ϵ:

$$
\begin{aligned}
\frac{r_{\text{area}}^{(2)}}{r} = \frac{1}{4} \operatorname{tr} \Bigg\{ & \boldsymbol{\gamma}_{(2)}(u_o) \cos\theta + \boldsymbol{\gamma}_{(2)}(u_s) - (1 + \cos\theta) \cos\theta \left[\langle \boldsymbol{\gamma}_{(2)} \rangle + \langle \boldsymbol{h} \rangle^2 - \langle \boldsymbol{h}^2 \rangle \right] \\
& + (1 - \cos\theta)[\langle \boldsymbol{h} \rangle - \boldsymbol{h}(u_o)]^2 - \frac{1}{2}[\boldsymbol{h}^2(u_o) + \boldsymbol{h}^2(u_s) - 2\langle \boldsymbol{h} \rangle^2] \Bigg\} + \left(\frac{u_s^{(1)}/\sqrt{2}r}{1 + \cos\theta} \right) \\
& \times \left[\frac{2\langle h_{ij} \rangle - h_{ij}(u_o) - h_{ij}(u_s)}{1 + \cos\theta} + \frac{1}{2}(3 + \cos\theta)\langle h_{ij} \rangle - h_{ij}(u_s) \right] \hat{k}_\perp^i \hat{k}_\perp^j.
\end{aligned} \tag{88}
$$

The second-order perturbation to the luminosity distance follows from this, (78), (80), and (86) via

$$
\frac{r_{\text{lum}}^{(2)}}{r} = \frac{r_{\text{area}}^{(2)}}{r} - 2\big(\omega_o^{(1)}/\omega_s\big) \frac{r_{\text{area}}^{(1)}}{r} + 3\big(\omega_o^{(1)}/\omega_s\big)^2 - 2\big(\omega_o^{(2)}/\omega_s\big). \tag{89}
$$

4.2.6. Summary of second-order effects Most terms in the second-order expressions derived above are relatively uninteresting in the sense that their magnitudes are comparable to squares of typical first-order magnitudes. If these latter $O(\epsilon)$ effects are only marginally detectible, their squares are hopelessly small. More interesting are the second-order terms that can acquire large numerical coefficients. As motivated in Section 4.1, $\boldsymbol{\gamma}_{(2)}$ can be large, thus implying that (77) and (85) simplify to

$$u_s^{(2)} = -\frac{r}{4\sqrt{2}} \operatorname{tr}\langle\boldsymbol{\gamma}_{(2)}\rangle \sin^2\theta + \dots, \tag{90}$$

$$\theta_{(2)} = \frac{1}{4} \operatorname{tr}\left\{\left[\langle\boldsymbol{\gamma}_{(2)}\rangle - \boldsymbol{\gamma}_{(2)}(u_o)\right] + \langle\boldsymbol{\gamma}_{(2)}\rangle \cos\theta\right\} \sin\theta + \dots, \tag{91}$$

at large distances. These are identical to the expressions which would be obtained if the first-order expressions (74) and (82) for $u_s^{(1)}$ and $\theta_{(1)}$ were applied with the substitution $\boldsymbol{h} \to \epsilon\boldsymbol{\gamma}_{(2)}$, providing a sense in which the potentially-significant contributions to u_s and θ through second order mimic first-order effects with an "effective first-order metric" $\boldsymbol{h} + \epsilon\boldsymbol{\gamma}_{(2)}$. This effective metric has a nonzero trace, and therefore mimics a third type of gravitational wave polarization.

Similar comments apply only to some of the potentially-large contributions to the second-order frequency perturbation (80). The trace terms in

$$\frac{\omega_o^{(2)}}{\omega_s} = \frac{1}{4}(1 - \cos\theta) \operatorname{tr}[\boldsymbol{\gamma}_{(2)}(u_s) - \boldsymbol{\gamma}_{(2)}(u_o)] + \frac{1}{2}\left(u_s^{(1)}/r\right)\left(\frac{r\dot{h}_{ij}(u_s)\hat{k}_\perp^i \hat{k}_\perp^j}{1 + \cos\theta}\right) + \dots \tag{92}$$

are indeed those which would be obtained by adding an appropriate correction to the metric perturbation appearing in $\omega_o^{(1)}/\omega_s$. The remaining portion of the second-order frequency perturbation is different, however. It arises from the wave-induced perturbation to the emission phase, and can be important when h_{ij} varies significantly over scales of order $\epsilon u_s^{(1)}$. Somewhat more precisely, use of (74) shows that the $\dot{h}_{ij}$ term in (92) can be large if $\langle h_{ij}\rangle$ is significant *and* there is a sense in which $r\dot{h}_{ij} \gg h_{ij}$. This occurs if, e.g., a gravitational wave possesses both high and low frequency components. See Section 5.3.

Second-order expressions for the area and luminosity distance are different from those associated with the other observables discussed here. Using (88) and (89), they are dominated by

$$\frac{r_{\text{area}}^{(2)}}{r} = \frac{1}{4} \operatorname{tr}\left[\boldsymbol{\gamma}_{(2)}(u_o)\cos\theta + \boldsymbol{\gamma}_{(2)}(u_s) - (1 + \cos\theta)\cos\theta\langle\boldsymbol{\gamma}_{(2)}\rangle\right] + \dots \tag{93}$$

and

$$\frac{r_{\text{lum}}^{(2)}}{r} = \frac{1}{4} \operatorname{tr}\left[(2 - \cos\theta)\boldsymbol{\gamma}_{(2)}(u_o) + (2\cos\theta - 1)\boldsymbol{\gamma}_{(2)}(u_s)\right.$$
$$\left. - (1 + \cos\theta)\cos\theta\langle\boldsymbol{\gamma}_{(2)}\rangle\right] - \left(u_s^{(1)}/r\right)\left(\frac{r\dot{h}_{ij}(u_s)\hat{k}_\perp^i \hat{k}_\perp^j}{1 + \cos\theta}\right) + \dots \tag{94}$$

at large distances. These results could not have been guessed by the use of an effective metric in the first-order perturbations (86) and (87). The difference terms are physically associated with the gravitational focusing of neighboring null geodesics.

5. Gravitational wave examples

We now consider three examples with which to illustrate some physical consequences of the perturbative expressions derived in Section 4. The first of these involves a gravitational wave which is both monochromatic and linearly-polarized. Next under discussion is a fast burst with nontrivial memory. Lastly, we consider a superposition of these two idealized waves.

5.1. Optics in a monochromatic wave

Perhaps the simplest physically-interesting gravitational wave is a linearly-polarized example whose curvature is monochromatic in the sense described in Section 4.1.2. Specifically, consider a family (45) of waves with curvatures given by (63). Also suppose that Rosen coordinates have been chosen such that $\boldsymbol{\gamma}_{(1)} = \boldsymbol{h}$ is given by (64) and $\boldsymbol{\gamma}_{(0)} = \boldsymbol{I}$.

The first-order frequency shift for coordinate-stationary sources and observers embedded in such a wave follows from (79):

$$\omega_o^{(1)}/\omega_s = \frac{1}{2}(\cos \omega u_o - \cos \omega u_s)(1 - \cos \theta) \cos 2\phi. \tag{95}$$

This generically oscillates with u_o, but vanishes for any sources with $\phi_{(0)}$ satisfying (76). The other observables depend on the average waveform $\langle h_{ij} \rangle$ between the emission and observation events. Using (73) to define the zeroth-order estimate

$$N \equiv \frac{\omega r}{2^{3/2}\pi}(1 + \cos \theta) \tag{96}$$

for the number of gravitational wave cycles between these events, $\langle h_{ij} \rangle \sim N^{-1}$ over large distances where $N \gg 1$. It follows that averages can be ignored at first order in the large-distance limit. Equation (74) then implies that $u_s^{(1)} \to 0$. The first-order position change is nontrivial, however, and may be described by

$$\theta_{(1)} \to \frac{1}{2} \cos \omega u_o \sin \theta \cos 2\phi, \qquad \phi_{(1)} \to -\frac{1}{2} \cos \omega u_o \sin 2\phi. \tag{97}$$

It also follows from (86) and (87) that the first-order perturbations to a source's apparent distance are

$$r_{\text{area}}^{(1)}/r \to \frac{1}{2}(1 - \cos \theta) \cos 2\phi \cos \omega u_o, \tag{98}$$

$$r_{\text{lum}}^{(1)}/r \to (1 - \cos \theta) \cos 2\phi (\cos \omega u_s - \frac{1}{2} \cos \omega u_o), \tag{99}$$

when $\langle h_{ij} \rangle \to 0$.

Continuing these calculations through second order, it follows from (65) that the dominant contribution to the waveform is

$$\boldsymbol{\gamma}_{(2)}(u) = -\frac{1}{8}(\omega u)^2 \boldsymbol{I} + \ldots \tag{100}$$

at large u. Substituting this into (92) results in

$$\omega_o^{(2)}/\omega_s = \frac{\pi^2 N^2}{4}\left[2\left(\frac{u_o}{u_o - u_s}\right) - 1\right](1 - \cos \theta) + \ldots. \tag{101}$$

The $\pi^2 N^2$ factor appearing here can be enormous at large distances, potentially allowing the magnitude of $\epsilon \omega_o^{(2)}$ to compete with $\omega_o^{(1)}$. The temporal and angular

dependencies of the first and second-order effects are very different, however. Similar comments also apply to the other observables considered here. Second-order averages $\langle \boldsymbol{\gamma}_{(2)} \rangle$ are not generically negligible at any distance. Computing this average for (100) and substituting into (91) shows that

$$
\begin{aligned}
\theta_{(2)} = \frac{\pi^2 N^2}{12} \Bigg\{ & \left[3 \left(\frac{u_o}{u_o - u_s} \right) - 1 \right] (1 + \cos\theta) \\
& - 3 \left(\frac{u_o}{u_o - u_s} \right)^2 \cos\theta \Bigg\} \sin\theta + \dots,
\end{aligned}
\tag{102}
$$

which is again proportional to $\pi^2 N^2$. Although the first-order observables oscillate for monochromatic waves, their second-order counterparts act (at least over short observation times) more like offsets. These offsets depend in a characteristic way on both the distance to a source and its angular separation from the wave propagation direction. Their magnitudes can be comparable to first-order effects when $N \sim \omega r \sim \epsilon^{-1/2}$.

5.2. Optics and the memory effect

As a second example, consider a quick burst of gravitational waves as described in Section 4.1.1. We do not model the burst itself, but only its memory in the form of the second-order Rosen waveform (61). Observations may then be split into three main phases. These are the i) early times where $u_o < -\delta$, ii) intermediate times where $u_o > 0$ but $u_s < -\delta$, and iii) late times where $u_s > 0$. The first and last of these phases involve light propagating entirely through flat regions of spacetime.

We start by considering first-order effects. The frequency shift is particularly simple, vanishing at both early and late times, and holding the constant value

$$
\omega_o^{(1)}/\omega_s = -\frac{1}{2}(1 - \cos\theta) \cos 2\phi
\tag{103}
$$

at intermediate times. The true frequency shift would not, of course, jump between these possibilities instantaneously. Transitions would instead last for observation times of order δ, and would depend on detailed properties of the burst. Additionally, this expression for $\omega_o^{(1)}$ does not vanish as $\theta_{(0)} \to \pi$ despite the general comments following (79). This is another artifact of the discontinuity introduced in the waveform by ignoring timescales of order δ.

Other observables depend on $\langle h_{ij} \rangle$, which cannot be ignored when memory effects are important. Indeed, this average imparts various observables with the "continuous component" of their time dependence. For example, (74) implies that $u_s^{(0)}$ is initially zero, changes linearly with u_o via

$$
u_s^{(1)} = -\frac{r}{2\sqrt{2}} \left(\frac{u_o}{u_o - u_s} \right) \sin^2\theta \cos 2\phi
\tag{104}
$$

at intermediate times, and then saturates to a constant value at late times.

Astrometric effects are somewhat more complicated. Through first order, a source which is initially stationary at $(\theta, \phi) = (\theta_{(0)}, \phi_{(0)})$ rapidly moves to a position determined by

$$
\theta_{(1)} = -\frac{1}{2} \sin\theta \cos 2\phi, \qquad \phi_{(1)} = \frac{1}{2} \sin 2\phi
\tag{105}
$$

when $u_o = 0$. These perturbations then vary linearly with u_o until saturating at

$$\theta_{(1)} = \frac{1}{4}\sin 2\theta \cos 2\phi, \qquad \phi_{(1)} = -\frac{1}{2}\sin 2\phi, \tag{106}$$

where they remain for all late times. That the asymptotic angular perturbations are nonzero is a consequence of the finite displacement memory associated with the gravitational wave.

The distance observables r_{area} and r_{lum} are both equal to r at early times. They then suffer the the equal and opposite first-order perturbations

$$r_{\text{lum}}^{(1)} = -r_{\text{area}}^{(1)} = \frac{1}{2}r(1 - \cos\theta)\cos 2\phi \tag{107}$$

when $u_o = 0$. These perturbations subsequently vary linearly with u_o until reaching

$$r_{\text{area}}^{(1)} = \frac{1}{2}r\sin^2\theta\cos 2\phi, \qquad r_{\text{lum}}^{(1)} = r_{\text{area}}^{(1)} + r(1 - \cos\theta)\cos 2\phi \tag{108}$$

when u_o approaches $r(1 + \cos\theta_{(0)})/\sqrt{2}$ from below. The perturbation to the area distance retains this value for all later times, while the perturbation to the luminosity distance instead jumps so as to agree (again) with $r_{\text{area}}^{(1)}$ at late times.

Continuing these calculations through second order, we focus on the contribution due to the constant $\text{tr}(\boldsymbol{b}_{\mathcal{F}_+})_{(2)}$ appearing in (61). As explained following (59), this constant must be negative if the first-order memory is to perturb only the asymptotic positions of test particles, and not their velocities. The relevant portion $\boldsymbol{\gamma}_{(2)}(u) = u[\text{tr}(\boldsymbol{b}_{\mathcal{F}_+})_{(2)}]\boldsymbol{I} + \dots$ of the second-order metric then contributes

$$\omega_o^{(2)}/\omega_s = -\frac{1}{2}u_o[\text{tr}(\boldsymbol{b}_{\mathcal{F}_+})_{(2)}](1 - \cos\theta) + \dots \tag{109}$$

to the frequency shift at intermediate times. This is nowhere negative, and therefore corresponds to a linearly-increasing blueshift. It is an effect which saturates at

$$\omega_o^{(2)}/\omega_s = -\frac{r}{2\sqrt{2}}[\text{tr}(\boldsymbol{b}_{\mathcal{F}_+})_{(2)}]\sin^2\theta + \dots, \tag{110}$$

where it remains for all late times. Gravitational wave bursts therefore induce permanent blueshifts at this order. Initially-comoving test particles are focused by the wave, experiencing a small "velocity memory" at late times. This is a nonlinear effect proportional to the nominal source-observer distance r.

Similarly considering the dominant large-distance effect on θ at second order, it follows from (91) that $\theta_{(2)}$ continuously changes from zero according to

$$\theta_{(2)} = \frac{1}{4}u_o[\text{tr}(\boldsymbol{b}_{\mathcal{F}_+})_{(2)}]\left[\left(\frac{u_o}{u_o - u_s}\right)(1 + \cos\theta) - 2\right]\sin\theta + \dots \tag{111}$$

at intermediate times. This is nowhere negative, indicating that second-order effects tend to make objects appear to bunch up against the wave propagation direction. This behavior transitions to

$$\theta_{(2)} = \frac{1}{4}(u_o - u_s)[\text{tr}(\boldsymbol{b}_{\mathcal{F}_+})_{(2)}]\left[2\left(\frac{u_o}{u_o - u_s}\right)\cos\theta - (1 + \cos\theta)\right]\sin\theta + \dots \tag{112}$$

at late times, the sign of which depends on $\theta_{(0)}$ and u_o. The late-time dependence of θ on u_o is another consequence of the velocity memory imparted by the gravitational wave burst at second order.

5.3. Superimposed bursts and continuous waves

Our last example consists of a superposition of the monochromatic and burst-type waves discussed above. Allowing the relative amplitudes of these components to differ by a constant factor h_∞, suppose that

$$\boldsymbol{h}(u) = [h_\infty \Theta(u) - \cos \omega u] \begin{pmatrix} 1 & 0 \\ 0 & -1 \end{pmatrix} \tag{113}$$

except in a small neighborhood of $u = 0$, where $\Theta(u)$ is equal to one for $u > 0$ and vanishes otherwise. All first-order perturbations to the optical observables in this case have the form (results of Section 5.1) $+ h_\infty \times$ (results of Section 5.2).

Second-order effects are potentially more interesting. In particular, the $\dot{h}_{ij}$ contributions to the frequency shift (92) and the luminosity distance (94) can be significant. Using (104) while assuming that the number of cycles (96) associated with the continuous wave satisfies $N \gg 1$, this reduces to

$$\frac{u_s^{(1)}}{r} \left(\frac{r \dot{h}_{ij}(u_s) \hat{k}_\perp^i \hat{k}_\perp^j}{1 + \cos \theta} \right) = -\pi N h_\infty (1 - \cos \theta)^2 \cos^2 2\phi \sin \omega u_s \tag{114}$$

at late times. Unlike the other second-order examples considered here, this oscillates with the same frequency as the first-order waveform. The prefactor $\pi N h_\infty$ can also be extremely large, particularly if the memory amplitude is much larger than the amplitude of the monochromatic component so $h_\infty \gg 1$.

6. Conclusions

We have derived exact time delays, frequency shifts, area and luminosity distances, and sky positions associated with optical observations in the presence of gravitational plane waves. One consequence is that the observed positions and frequency shifts associated with moving objects effectively use osculating geodesics to extrapolate source-observer separations to "simultaneous times." Another result is that the functional form for the well-known linearized frequency shift is nearly identical to the exact frequency shift when observers and sources both move on geodesics adapted to a Rosen coordinate system. The only explicit change is that the difference $\boldsymbol{h}(u_s) - \boldsymbol{h}(u_o)$ between metric perturbations at the emission and observation events which appears in the approximate result is replaced by $\boldsymbol{\xi}(u_o)[\boldsymbol{\gamma}^{-1}(u_o) - \boldsymbol{\gamma}^{-1}(u_s)]\boldsymbol{\xi}^{\mathsf{T}}(u_o)$. This involves the "square root" ξ_{ij} of the full transverse Rosen metric $\gamma_{ij} = \xi_{ki}\xi_{kj}$ only at $u = u_o$ and $u = u_s$.

More generally, most of our exact results would be awkward to write in terms of deviations away from a flat background. They are very simple, however, in terms of ξ_{ij}. Einstein's equation is also relatively simple in terms of this variable, reducing to linear differential equations analogous to those which describe a set of parametric oscillators whose couplings are proportional to the spacetime curvature. ξ_{ij} is closely related to the Jacobi propagators which determine solutions to the geodesic deviation equation, and can also be compared to a tetrad representation for the metric. While some results following from the use of this variable are peculiarities of the plane wave geometry, similar choices might nevertheless simplify optical calculations in more general spacetimes.

Our main physical discussion has focused on the large-distance behavior of γ_{ij} and its associated optical effects. For clarity and ease of comparison to earlier work, this was investigated mainly using perturbative expansions. Assuming a regular expansion

controlled by a wave's curvature, the first-order metric perturbation $h_{ij} = \gamma_{ij}^{(1)}$ is easily arranged to be an ordinary TT-gauge waveform. Indeed, the traces of all odd-order metric perturbations can be arranged to vanish. This does not generalize to even orders, however. For every even $n \geq 2$, the trace of the nth-order metric perturbation is generically nonzero, and furthermore, $\gamma_{ij}^{(n)} = \frac{1}{2}(\operatorname{tr}\boldsymbol{\gamma}_{(n)})\delta_{ij}$. These distinct properties are reflected in very different angular dependencies for the optical effects induced by, e.g., the first and second-order metric perturbations. In many ways, nonlinear effects act like effective trace corrections to h_{ij} which mimic a third, "breathing"-type gravitational wave polarization mode. Such effects might complicate efforts [47] to constrain alternative theories of gravity where—unlike in general relativity—breathing modes arise as true, physically-independent degrees of freedom.

The second-order metric which typically provides the dominant trace contribution in general relativity is governed by a double integral of the "gravitational wave energy density" $\dot{\boldsymbol{h}}^2$. This density is non-negative, so its integrals tend to grow rapidly with distance. For the special case of a monochromatic wave with constant amplitude (at least over the relevant timescales), $\operatorname{tr}\boldsymbol{\gamma}_{(2)}$ scales with the square of the number of curvature oscillations N. This number is not large for the waves intended to be observed using standard interferometer designs—arm lengths in those cases are not large compared to wavelengths. Nonlinear effects are potentially more interesting in connection with pulsar timing or related observations, although their detection would still be challenging. For example, the amplifying prefactor appearing in the second-order frequency shift (101) is $N^2 \sim 10^{11}$ for observations of a pulsar $r \sim 10\,\mathrm{kpc}$ away in the presence of a gravitational wave with frequency $\omega/2\pi \sim 300\,\mathrm{nHz}$. Multiplying this by a reasonable strain magnitude unfortunately results in a second-order effect which is still quite small. Although its unusual angular dependence improves detectability, any such improvement is likely offset by its time dependence. With the exception of the effect described in Section 5.3, large second-order terms do not oscillate. They instead contribute polynomial time dependencies with coefficients which depend on the distance to a source and its orientation with respect to the gravitational wave. Practical pulsar timing observations must take into account a number of effects beyond those explicitly described here, and therefore fit their data to a model. As-is, these fits would likely eliminate all interesting contributions associated with second-order metric perturbations. It may therefore be more favorable to consider measurement scenarios where source frequencies can be locally (and nonlocally) measured to high accuracy.

The unusual time-dependence of the nonlinear terms considered here can also be viewed as a positive feature. Waves whose linear features are at frequencies too high to be seen directly with a particular detector might nevertheless be observable via their nonlinearities. Indeed, higher frequencies tend to produce larger effects for a fixed strain amplitude and distance.

Acknowledgments

References

[1] Pitkin M et al. 2011 *Living Rev. Relativity* **14** 5

[2] Hobbs G et al. 2010 *Class. Quantum Grav.* **27** 084013
[3] Harte A I 2013 *Class. Quantum Grav.* **30** 075011
[4] Book L G and Flanagan É É 2011 *Phys. Rev. D* **83** 024024
[5] Zipoy D M 1966 *Phys. Rev.* **142** 825
[6] Damour T and Esposito-Farése G 1998 *Phys. Rev. D* **58** 044003
[7] Kopeikin et al. 1999 *Phys. Rev. D* **59** 084023
[8] Faraoni V 2008 *New Astron.* **13** 178
[9] Faraoni V 1991 *Gen. Rel. Grav.* **23** 583
[10] Helfer A D 2013 *Mon. Not. R. Astr. Soc.* **430** 305
[11] Koop M J and Finn L S 2014 *Phys. Rev. D* **90** 062002
[12] Perlick V 2004 *Living Rev. Relativity* **7** 9
[13] Bičak J et al. 2012 *Phys. Rev. D* **85** 124003
[14] Detweiler S 1979 *Astrophys. J.* **234** 1100
[15] Kopeikin S, Korobkov P and Polnarev A 2006 *Class. Quantum Grav.* **23** 4299
[16] Brügmann M H 2005 *Phys. Rev. D* **72** 024012
[17] Hees A, Bertone S and Le Poncin-Lafitte C 2014 *Phys. Rev. D* **89** 064045
[18] Penrose R 1976 Any spacetime has a plane wave as a limit *Differential Geometry and Relativity* ed M Cahen and M Flato (Dordrecht: Reidel)
[19] Blau M, Frank D and Weiss S 2006 *Class. Quantum Grav.* **23** 3993
[20] Harte A I and Drivas T D 2012 *Phys. Rev. D* **85** 124039
[21] Misner C W, Thorne K S and Wheeler J A 1973 *Gravitation* (San Francisco, CA: Freeman)
[22] Wald R M 1984 *General relativity* (Chicago, IL: University of Chicago Press)
[23] Flanagan É É and Hughes S A 2005 *New J. Phys.* **7** 204
[24] Bondi H, Pirani F A E and Robinson I 1959 *Proc. Roy. Soc. London* A **251** 519
[25] Ehlers J and Kundt W 1962 *Gravitation: An introduction to current research*, ed. Witten L (New York, NY: Wiley)
[26] Xanthopoulos B C 1978 *J. Math. Phys.* **19** 1607
[27] Synge J L 1966 *Relativity: The general theory* (Amsterdam: North-Holland)
[28] Wu S-M and Shih C-C 1985 *Phys. Rev. A* **32** 3736
[29] Takayama K 1986 *Phys. Rev. A* **34** 4408
[30] Magnus W and Winkler M 1979 *Hill's Equation* (New York, NY: Dover)
[31] Poisson E, Pound A and Vega I 2011 *Living Rev. Relativity* **14** 7
[32] Friedlander F G 1975 *The wave equation on a curved spacetime* (Cambridge: Cambridge University Press)
[33] Le Poncin-Lafitte C, Linet B and Teyssandier P 2004 *Class. Quantum Grav.* **21** 4463
[34] Faraoni V 1998 *Int. J. Mod. Phys.* D **7** 409
[35] Creighton T, Jenet F A, and Price R H 2009 *Astrophys. J.* **693** 1113
[36] Estabrook F B and Wahlquist H D 1975 *Gen. Rel. Grav.* **6** 439
[37] Vutha A *arXiv*:1501.01870
[38] Armstrong J W 2006 *Living Rev. Relativity* **9** 1
[39] Isaacson R A 1968 *Phys. Rev.* **166** 1263; *Phys. Rev.* **166** 1272
[40] Burnett G A 1989 *J. Math. Phys.* **30** 90
[41] Braginsky V B and Grischuk L P 1985 *Sov. Phys. JETP* **62**, 427
[42] Braginsky V B and Thorne K S 1987 *Nature* **327** 123
[43] Bieri L and Garfinkle D 2013 *Class. Quantum Grav.* **30** 195009
[44] Grischuk L P and Polnarev A P 1989 *Sov. Phys. JETP* **69** 653
[45] Bessonov E G 1981 *Sov. Phys. JETP* **53** 433
[46] Faraoni V 1996 *Astrophys. Lett. Comm.* **35** 305
[47] Lee K J, Jenet F A and Price R H 2008 *Astrophys. J.* **685** 1304